



Contents lists available at ScienceDirect

## Expert Systems With Applications

journal homepage: [www.elsevier.com/locate/eswa](http://www.elsevier.com/locate/eswa)

## SIMCD: SIMulated crowd data for anomaly detection and prediction

Amna Bamaqa<sup>a,b,\*</sup>, Mohamed Sedky<sup>a,2</sup>, Tomasz Bosakowski<sup>a,3</sup>, Benhur Bakhtiari Bastaki<sup>a,4</sup>, Nasser O. Alshammari<sup>c,5</sup><sup>a</sup> School of Digital, Technologies and Arts, Staffordshire University, Stoke-on-Trent ST4 2DE, UK<sup>b</sup> Department of Computer Science and Information, Applied College, Taibah University, Medina, Saudi Arabia<sup>c</sup> Department of Computer Science, College of Computer and Information Sciences, Jouf University, Saudi Arabia

## ARTICLE INFO

## Keywords:

Synthetic data  
Real data  
Datasets  
Internet of things  
Crowd management  
Crowd model  
Simulation  
Machine learning  
Prediction  
Anomaly detection

## ABSTRACT

Smart Crowd management (SCM) solutions can mitigate overcrowding disasters by implementing efficient crowd learning models that can anticipate critical crowd conditions and potential catastrophes. Developing an SCM solution involves monitoring crowds and modelling their dynamics. Crowd monitoring produces vast amounts of data, with features such as densities and speeds, which are essential for training and evaluating crowd learning models. By and large, crowd datasets can be classified as real (e.g., real monitoring of crowds) or synthetic (e.g., simulation of crowds). Using real crowd datasets can produce effective and reliable crowd learning models. However, acquiring real crowd data faces several challenges, including the expensive installation of a sensory infrastructure, the data pre-processing costs and the lack of real datasets that cover particular crowd scenarios. Consequently, crowd management literature has adopted simulation tools for generating synthetic datasets to overcome the challenges associated with their real counterparts. The majority of existing datasets, whether real or synthetic, can be used for crowd counting applications or analysing the activities of individuals rather than collective crowd behaviour. Accordingly, this paper demonstrates the process of generating bespoke synthetic crowd datasets that can be used for crowd anomaly detection and prediction, using the MassMotion crowd simulator. The developed datasets present two types of crowd anomalies; namely, high densities and contra-flow walking direction. These datasets are: SIMulated Crowd Data (SIMCD)-Single Anomaly and SIMCD-Multiple Anomalies for anomaly detection tasks, besides two SIMCD-Prediction datasets for crowd prediction tasks. Furthermore, the paper demonstrates the data preparation (pre-processing) process by aggregating the data and proposing new essential features, such as the level of crowdedness and the crowd severity level, that are useful for developing crowd prediction and anomaly detection models.

## 1. Introduction

A crowd is a large gathering of people for either predefined (e.g., sports or pilgrimage events) or spontaneous (e.g., random gathering by chance or coincidence) purposes. Helbing and Johansson (2013) defined a crowd as an “Agglomeration of many people in the same area at the same time. The density of people is assumed to be high enough to cause continuous interactions, or reactions, with other individuals.” The

density, flow and speed of movement are the main characteristics of a crowd that can determine its critical condition (Johansson, Helbing, Al-Abideen, & Al-Bosta, 2008b). Crowd density defines the number of people per unit area at a particular time (Helbing & Johansson, 2013; Schauer, Werner, & Marcus, 2014). The density and speed govern the crowd flow rate; an increase in the crowd density slows the movement speed and vice versa (Smith, 1995). Crowd disasters can result from individuals’ behaviour, such as space-seeking or panic or from the

\* Corresponding author.

E-mail addresses: [b012746g@student.staffs.ac.uk](mailto:b012746g@student.staffs.ac.uk) (A. Bamaqa), [M.H.Sedky@staffs.ac.uk](mailto:M.H.Sedky@staffs.ac.uk) (M. Sedky), [T.Bosakowski@staffs.ac.uk](mailto:T.Bosakowski@staffs.ac.uk) (T. Bosakowski), [b.b.bastaki@staffs.ac.uk](mailto:b.b.bastaki@staffs.ac.uk) (B. Bakhtiari Bastaki), [nashamri@ju.edu.sa](mailto:nashamri@ju.edu.sa), [aa20006@hotmail.com](mailto:aa20006@hotmail.com) (N.O. Alshammari).

<sup>1</sup> <https://orcid.org/0000-0001-6576-7956>.<sup>2</sup> <https://orcid.org/0000-0002-9169-2449>.<sup>3</sup> <https://orcid.org/0000-0002-1646-0429>.<sup>4</sup> <https://orcid.org/0000-0003-3420-7299>.<sup>5</sup> <https://orcid.org/0000-0003-4374-3675>.<https://doi.org/10.1016/j.eswa.2022.117475>

Received 17 January 2022; Received in revised form 25 April 2022; Accepted 28 April 2022

Available online 2 May 2022

0957-4174/© 2022 The Author(s). Published by Elsevier Ltd. This is an open access article under the CC BY license (<http://creativecommons.org/licenses/by/4.0/>).

breakdown of co-ordination, such as the removal of physical barriers. Pedestrians' interactions in a crowd do not adhere to previously agreed rules or regulations. Their movements, governed by self-organising motion patterns, shape the form of crowd flow (e.g., lane formation, stop and go waves or turbulence). Thus, a crowd could occur anywhere at any time after reaching a specific density or following a disruption in speed and flow.

Overcrowding (*a.k.a.* congestion or dense crowding) occurs when the number of people exceeds the level that can be comfortably accommodated. The potential for overcrowding happens daily at a variety of locations such as transport hubs (Toto, Rundensteiner, Li, Jordan, Ishutkina, Claypool, & Zhang, 2016), large events (such as pilgrimage) (Felemban et al., 2020) and also in urban areas (Wu, Dong, Huang, Xu, Wang, & Chawla, 2017; Zhang et al., 2020). Overcrowding without an efficient crowd management system can lead to dangerous congestion or stampede resulting in injury or death (Franke, Lukowicz, & Blanke, 2015; Helbing & Mukerji, 2012). For example, the absence of an effective crowd management system during a large pilgrimage event resulted in excessive congestion and significant loss of life (BBC, 2015). This emphasises the need for crowd management solutions for large-scale events as well as daily activities to ensure people's safe, smooth movement.

Large crowds are influenced by a range of physical and socio-psychological characteristics (dynamic features) arising from different crowd behaviour and result in different normal or abnormal behaviour (Challenger, Clegg, & Robinson, 2009; Zitouni, Sluzek, & Bhaskar, 2019). For example, density and flow measurements differ based on demographic and geographic characteristics, which, in turn, affect the design of facilities and the assessment of capacity restrictions when holding large-scale events in different countries (Helbing & Johansson, 2013). The literature identifies several characteristics that describe crowd motion patterns. These characteristics include the dimension or spatial information (e.g., area, number of pedestrians and density), movements or temporal information (e.g., speed and acceleration), velocity or spatial-temporal information (e.g., direction and flow rate) and social behaviour (e.g., crowd activities) (Draghici & Steen, 2018). Hence, different standards define typical behaviour for different crowd types (Helbing, Farkas, Molnar, & Vicsek, 2002).

Understanding crowd dynamics and the implications of crowd characteristics contributes to decision making in artificial intelligence applications, indicating critical or undesirable situations that can be predicted and avoided (Helbing & Johansson, 2013) (Helbing, Buzna, Johansson, & Werner, 2005). There is ample evidence in the literature to confirm that early detection of changes in crowd behaviour, such as unstable flow, decreased speed, or increased density, can be used to predict adverse situations (Helbing et al., 2015). Accurate prediction relies on analysis of interactions, cascade effects and feedback loops (Franke et al., 2015; Wirz et al., 2012). Crowd management solutions monitor the state of the crowd and the changes in movement patterns to differentiate between normal and abnormal crowd patterns. Over the past decade, crowd management research has focused on the use of visual crowd analysis techniques to analyse videos from closed-circuit television (CCTVs) (Khan, Albattah, Khan, Qamar, & Nayab, 2020; Zhang, Yu, & Yu, 2018). Technological advances show considerable promise for collecting this relevant crowd data providing robust and realistic datasets for future research. Smart Crowd Management (SCM) systems integrate the Internet of Things (IoT) and Machine Learning (ML) technology which leverage the intelligence and efficiency of crowd management process (Felemban et al., 2020; Kaiser et al., 2018). This technology automatically senses, collects, transmits, analyses, and infers semantic content of crowd data, which is based on density estimation, prediction and anomaly detection techniques. SCM systems dynamically adapt to changes in crowd conditions, identify anomalies and provide early warning signs by recognising subtle changes and developments in crowd patterns. SCM systems use crowd data to train, test and validate crowd prediction and anomaly detection models by applying

sophisticated pattern recognition and exploring correlations within the data (Zhang et al., 2020).

Crowd datasets and their characteristics play a vital role in building intelligent and robust learning models while allowing subsequent datasets to update or modify the models. More specifically, the choice of crowd dataset characteristics, such as density, direction or speed, can significantly affect the performance of crowd management models (Assem & Osullivan, 2017; Johansson, Helbing, Al-Abideen, & Al-Bosta, 2008a). Crowd management research uses either real or synthetic crowd datasets (Ruggiero, Charitha, Xiang, & Lucia, 2018; Schauer et al., 2014). The real crowd datasets are either generated or collected manually or automatically, using static or mobile sensing infrastructures (such as video surveillance recorders, location-motion sensing and radio-frequency signals) (Saleh, Suandi, & Ibrahim, 2015). These datasets represent different tasks and scenarios, but due to the natural scarcity of crowd anomalies the majority of such datasets are of limited value in the development of crowd management solutions. Real datasets have additional inherent challenges, including low-quality (e.g., missing data or poor lighting conditions), variety (e.g., limited scenarios), sensors installation challenges (e.g., weather conditions), size (usually small-scale) and limited accessibility (Draghici & Steen, 2018; Khan et al., 2020). Moreover, field experiments for generating real crowd datasets are not easy to conduct due to the cost and complexity of the situation to be modelled (e.g., fast-paced and rapidly developing situations and aggressive crowds) (Boltes, Adrian, & Raytarowski, 2021). Other challenges include considering the contextual aspects while adhering to ethical issues in emergency cases (Celes, Boukerche, & Loureiro, 2019; Haghani & Sarvi, 2018; Kaiser et al., 2018; Xie et al., 2020). With such challenges in collecting real crowd datasets, empirical research in the crowd analysis field lags behind the theoretical developments (Haghani & Sarvi, 2018).

The crowd management literature reports on the use of simulation tools that can significantly reduce the time required to generate scenario-specific crowd datasets that mimic observed crowds in a realistic environment, facilitate data-driven research and build functional (online or offline) machine learning models (Khadka et al., 2019). Simulation offers flexibility in adjusting the crowd scenarios, generating and reproducing bespoke datasets that meet the specified crowd scenario requirements (Amirian, Hayet, van Toll, & Pettré, 2019; Caramuta et al., 2017). However, most of the current simulated and real datasets are visual, used for counting tasks, or non-visual, for individual human activity recognition. There is a lack of crowd anomaly detection datasets (Bendali-Braham, Weber, Forestier, Idoumghar, & Muller, 2021; Khan et al., 2020; Luque Sánchez, Hupont, Tabik, & Herrera, 2020; Wang, Gao, Lin, & Yuan, 2019; Zhang et al., 2018). Accordingly, this paper demonstrates a case study using MassMotion simulation tool to generate viable synthetic crowd datasets based on the pre-specified crowd scenarios. This paper introduces four crowd datasets: SIMulated Crowd Data (SIMCD)-Single Anomaly, SIMCD-Multiple Anomalies, SIMCD-Prediction 1 and SIMCD-Prediction 2. These simulated datasets can be used in the context of crowd anomaly detection and prediction applications. For example, the proposed SIMCD datasets have already been adopted for evaluating crowd anomaly detection and prediction models (Bamaqa, Sedky, Bosakowski, & Bastaki, 2020; Bamaqa, Sedky, & Bastaki, 2022).

This paper is organised as follows: Section 2 discusses the related work of crowd management domain, including crowd behaviour and characteristics, real crowd data sources and datasets, simulation tools and synthetic crowd datasets, identifying the limitations of the current crowd anomaly detection datasets. Section 3 explains the underlying reasons for choosing the MassMotion simulator to simulate crowd movements while Section 4 details the entire workflow of generating the crowd dataset using MassMotion and the preparation phase to make the data ready for the prediction and anomaly detection models. Finally, Section 5 concludes the work.

## 2. Related work

The crowd management literature identifies different features, such as speed and direction, that characterise crowd movements (Draghici & Steen, 2018; Kaiser et al., 2018). Each crowd application, such as counting or density estimation, tracking, behaviour recognition, classification and anomaly detection, may be built using different crowd datasets that exhibit a subset of crowd features. Generally, crowd datasets can be collected or generated from real or synthetic sources. Real data is generated by using infrastructure-based sensors (such as static cameras) or application-driven (such as social media apps) data gathering methods (Draghici & Steen, 2018). Synthetic data are commonly generated using crowd simulation tools (Caramuta et al., 2017; Dubroca-Voisin, Kaban, & Leurent, 2019; Yang, Li, Gong, Peng, & Hu, 2020) or data-driven approaches by using machine learning to generate crowd data (Amirian et al., 2019; Khadka et al., 2019). The remainder of this section initially explains the *crowd behaviour and characteristics*, and then investigates the *real* and *synthetic* data sources and datasets in the crowd literature.

### 2.1. Crowd behaviour and characteristics

Haghani and Sarvi (2018) identified several issues in understanding normal and unexpected crowd behaviour, making it difficult to control the crowd and subsequently impact crowd models. For example, pedestrian behaviour is unpredictable and can vary significantly, even in the same situation. This makes the development of universal governing rules for pedestrian behavior complex and difficult to apply. In addition, pedestrian movements are flexible; completely different to vehicular movement which is governed by the road network structure and driving regulations. Moreover, from a geometric perspective, and compared to universal features of urban road structures, pedestrian geometrics are highly flexible regarding the diverse topologies, regions and crowd density. Changes in crowd context (e.g., crowd size and goal) affect human behaviour. For example, the behaviour of a very large crowd is dissimilar to small or medium counterparts. Additionally, the goal of the crowd has a direct impact in differentiating its normal from abnormal behaviour (e.g., the difference between a political protest and a musical festival).

Fig. 1 exhibits the relationship between the risk level of crowd densities (low and high) and the flow rate. Clearly, densities of up to two or three people per square metre with a flow of up to 82 people/metre/minute constitutes a low crowd risk. In contrast, critical cases occur when the density is more than four persons per square metre regarded as a high-risk density. Different density levels require different levels of response and, consequently, receive different *levels of services* (Fruin,

1987; Kretz, 2011; Polus, Schofer, & Ushpiz, 1983). Importantly, the density of a counterflow crowd is of greater significance than that of a uni-flow crowd (Wirz et al., 2013). In addition, a stationary crowd can reach a higher density before the situation becomes critical. As an illustration, the number of people per square metre increases by almost 50% (3.75 vs. 2.14) when sitting compared to walking (Abuarafah, Khoziun, & AbdRabou, 2012; Neufert, 2002).

Efforts to calculate the degree of crowdedness or congestion typically focus on density measures. However, other factors can also result in crowd congestion. Different cultures could lead to different speed-density relationships in the same setting (Dias, 2015). On occasion, the density in a critical situation is similar to that in safe conditions. Therefore, it is important to consider not only the density of a crowd but other conditions such as its location, speed, direction and behaviour (Feliciani & Nishinari, 2018). The crowd management literature has examined the relationship between pedestrian density, walking speed and flow, and has addressed normal and critical density levels (Ibrahim, Venkat, Subramanian, Khader, & Wilde, 2016; Vermuyten, Beliën, De Boeck, Reniers, & Wauters, 2016). These studies confirm an inverse relationship between density and speed, as described in Section (4.1.2), but also reveal variations in speed and density values due to the different standards adopted for defining typical crowd behaviour. While investigating congestion in dense crowds Khan (2019) observed a relationship between motion oscillation and average speed, greater oscillations leading to lower speeds over shorter distances. In contrast, free movement leads to longer, more predictable pathways for individuals and crowds. Unexpected situations involving heavy traffic and congestion which restrict, or even eliminate, free movement, can directly lead to conflict (Khan, 2019).

### 2.2. Real crowd data sources and datasets

There are two main approaches to collecting real crowd data: manual (expensive and error-prone) and automated (less expensive and more accurate). Automated methods are built on sensing capabilities to collect crowd data, classified into infrastructure-based (network) and application-driven (devices) (Draghici & Steen, 2018). The infrastructure-based real data collection methods use pre-installed static sensors, including visual (e.g., CCTV) (Saleh et al., 2015) or non-visual (e.g., acoustic, Wi-Fi) (Schauer et al., 2014). Conversely, application-driven data collection makes use of mobile on-board (visual and non-visual) sensing (e.g., GPS for location and accelerometer for motion) or software sensing (e.g., Twitter) to provide real-time updates of crowd conditions such as location, speed and direction (Felemban et al., 2020; Mohamed, Shabayek, & El-Gayyar, 2019). Taking advantage of the proliferation of mobile sensing and IoT technologies to collect crowd-

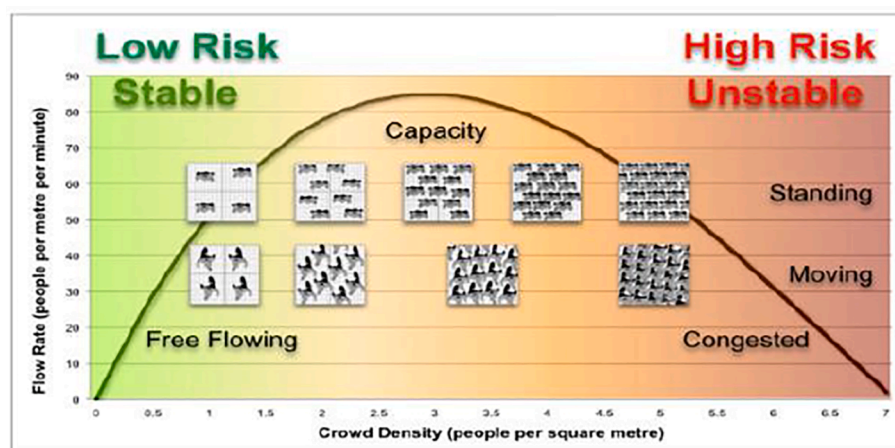


Fig. 1. Relationship between crowd density and flow rate (Still, 2011).

related data opens novel opportunities to manage the crowd promptly and improve situational awareness. A growing trend in fusing visual and non-visual sensors to capture real-world datasets is effective in large scale events to reflect accurate global assessment (e.g., crowd size and behaviour) and support informed decisions making (Kaiser et al., 2018; Li et al., 2021). In addition, real crowd data gathering methods can be divided based on user involvement: participatory, where users are consenting, active participants (Franke et al., 2015); or opportunistic, where users are passive participants (Higuchi, Yamaguchi, & Higashino, 2015). Many of the above crowd collection methods can be combined to achieve more accurate crowd classification, detection and prediction (Li et al., 2021).

Examples of real crowd, visual and non-visual, datasets are used in crowd related applications such as counting, density estimation, classification, activity recognition and anomaly detection. Most visual real crowd datasets have been targeting counting tasks such as *UCSD* (Chen, Liang, & Vasconcelos, 2008), *PETS2009* (Ferryman & Shahrokni, 2009), *UCF-CC-50* (Idrees, Saleemi, Seibert, & Shah, 2013), *Mall* (Chen, Loy, Gong, & Xiang, 2012), *Shanghai Tech* (Zhang, Zhou, Chen, Gao, & Ma, 2016), *WorldExpo'10* (Zhang et al., 2016), *NWPU-crowd* (Wang, Gao, Lin, & Li, 2020) and *JHU-CROWD++* (Sindagi, Yasarla, & Patel, 2020). **The UCSD dataset** is typical for crowd counting systems. Its 2000 images record pedestrian traffic over a one-hour period. **The PETS2009 dataset** is a collection of films using sequences captured by multiple cameras in real-world conditions and represents a variety of crowd activities. **The UCF-CC-50** is a dataset collected from Flickr. It contains 50 images with varying resolutions representing extremely dense crowds such as pilgrimages, marathons and in stadiums. **The Mall dataset** was collected from a publicly accessible webcam for crowd counting and profiling research and covers realistic crowded scenarios differing in terms of crowd density and activity. Ground truth consists of annotating 60,000 pedestrians into 2000 video frames with a resolution of  $640 \times 480$ . However, these crowd counting datasets have covered limited scenarios in a small-scale (limited number of samples and annotations) and therefore are unsuitable for building deep convolutional neural network-based models. To address this matter, **the Shanghai Tech dataset** was developed to be used when it is necessary to count large crowds. In total there are 330,165 annotated heads and 1,198 images, thereby making it among the largest datasets available for training and evaluation. The data consists of 482 images obtained from the Internet and a further 716 images taken of a Shanghai street. **The World Expo'10 crowd dataset** is another extensive dataset which was obtained from two hundred and forty-five closed-circuit cameras recording 2,630 videos at the 2010 World Expo in Shanghai. The videos cover a wide selection of scenes and the footage is well-suited for analysing cross-scene surveillance and estimating the crowd's density, segmentation, cohesiveness, and collectiveness. **NWPU** compiled a crowd dataset that utilises localisation and crowd counting and includes approximately 5,000 images and 2,133,375 annotated heads. **JHU-CROWD++** crowd datasets for counting cover a variety of scenarios (e.g., low, medium or high density) in different situations, geographical locations, under weather conditions such as fog, haze, snow and rain. **JHU-CROWD++** provides two levels of annotations; image-level, detailing the situation and weather; and head-level labelling which includes an approximate bounding box, dots, and degree of blurring.

Visual datasets are also used for understanding the behaviour of crowd dynamics, such as Activity recognition, anomaly detection and classification. Examples of these datasets include *UMN* (Mehran, Oyama, & Shah, 2009), *UCSD* (Li, Mahadevan, & Vasconcelos, 2013), *UCF* (University of Central Florida. (2011a), 2011a), *HUER* (Zawbaa & Aly, 2012), *Violent-Flows* (Hassner, Itcher, & Kliper-Gross, 2012), *Collective Motion* (Zhou, Tang, & Wang, 2013), *CUHK* (Shao, Loy, & Wang, 2014), *WWW* (Shao, Kang, Loy, & Wang, 2015) and *Crowd-11* (Dupont, Tobias, & Luvison, 2017). The University of Minnesota **UMN dataset** is a publicly available dataset for anomaly detection applications (Liu, Hao, Tang, & Wang, 2019; Mehran et al., 2009) consisting of normal and

abnormal crowd videos with indoor and outdoor scenarios. Panic situations are represented as anomalies. It consists of eleven videos; each one starting with people walking normally but ending with multiple normal and abnormal behaviour (panic movement). Another anomaly detection dataset, **the UCSD dataset** is also publicly available and contains a set of videos derived from a fixed-point camera located above the walkway at the University of California. The 98 videos represent both sparse and heavy pedestrian traffic. While training data represents normal cases (i.e., only pedestrians), testing data consists of normal and abnormal scenarios such as non-pedestrian objects (e.g., cars) or anomalies in pedestrian motion pattern (e.g., people riding scooters or bikes or walking across a walkway). These naturally occurring abnormal events make the dataset suitable for anomaly detection services. **The UCF datasets** represent multiple records of crowd motion, behaviour and actions include UCF101, UCF50, UCF11, YouTube Action and UCF Sports Action. The datasets were collected at the University of Central Florida from crowds with differing densities and perspectives. These datasets serve in a range of crowd applications such as human actions, crowd counting, segmentation and tracking. **The HUER (Hajj and Umrah Event Recognition) datasets** contain still and video images of different types of ritual events during Hajj and Umrah as well as videos and images of ordinary human actions during Hajj and Umrah, it aims to detect abnormal behaviour in Hajj and Umrah events, such as sitting or sleeping on sidewalks or stairs. **The Violent-Flows dataset** contains real-world video clips of crowd violence that has been assembled from YouTube. It demonstrates how crucial it is to detect violence very quickly in a crowded area to avoid a disaster. **The Collective Motion database** of 413 videos is used to gauge 'collectiveness': the extent to which people in crowds move collectively. **The CUHK Crowd dataset** provides various definitions of the ways in which crowds develop, such as intra-group stability and inter-group conflict. The 474 videos of crowds of different size and density are observed in a range of settings including shopping centres, high streets, parks and airports. It is categorised into classes including: highly mixed walking, well organised main stream, poorly organised main stream, crowd merging, crowd splitting, crossing in opposite directions, intervened escalator traffic and smooth escalator traffic. **WWW Crowd Dataset** is a comprehensive crowd dataset collected from different search engines and surveillance systems. It is available for research purposes and consists of 10,000 videos and 94 attributes in different scenarios. **The Crowd-11 dataset** was created to provide a large volume of labelled data with highly generic crowd behaviour which would meet the requirements of deep learning methods (e.g., CNN). The 6,272 video sequences are divided into: (1) crowds forming collective groups and (2) crowds without perceivable streams. The Crowd-11 dataset has eleven classes that have been manually selected from the Web and other datasets such as WWW and Violent-Flow.

As well as visual data, the crowd literature also introduces several examples of *non-visual* real crowd datasets, such as *CenceMe (Lite)* (Musolesi, Fodor, Piraccini, Corradi, & Campbell, 2008), *Nodobo* (Bell, McDiarmid, & Irvine, 2011), *Data for Development (D4D)* (Blondel, Esch, Chan, Clérot, Deville, & Huens, 2012), the *largest Swiss event* dataset (Blanke, Tröster, Franke, & Lukowicz, 2014), *non-visual crowd* dataset (Irfan, Tokarchuk, Marcenaro, & Regazzoni, 2018). **The CenceMe (Lite)** dataset was collected using a participatory mobile app carried by 20 participants for three weeks. The dataset size is approximately 252 MB and includes raw accelerometer data and GPS location coordinates for each user. The dataset aims to recognise the activity of humans by using mobile sensing to share location history and context information. **The Nodobo** dataset was collected from 27 high-school students from September 2010 to February 2011 using the Nodobo app. Nodobo dataset contains social context data including log data, call records (13035) and message records (83542). **The Data for Development (D4D)** dataset was collected anonymously from five million Orange mobile phone participants during a five-month period based on Call Detail Records (CDR) of the phones. CDRs includes the timestamp, caller

ID, callee ID, call duration, and the antenna code. [Blanke et al. \(2014\)](#) collected data for 28,000 visitors who attended the largest Swiss event, **Zuri Fascht** in 2013. The data collection experiments were carried out at the Performance Lab of Queen Mary University of London. The collected data includes information about visitors' location, speed, direction and time of location acquisition. The data represents 25 M location updates that capture crowd densities and flow. [Irfan et al. \(2018\)](#) created a real **non-visual crowd dataset** by monitoring participants at a social gathering event. This dataset was collected with the help of the Crowd sense application to capture any abnormal behaviour of participants. The data was collected using smartphones embedded with accelerometers and gyroscopes.

### 2.3. Simulation tools and synthetic crowd datasets

Synthetic data generation methods using crowd modelling and simulation tools can significantly reduce the time and cost required to generate scenario-specific crowd datasets. Most crowd models are based on assumptions, intuition and literature and many reflect specific scenarios ([Dubroca-Voisin et al., 2019](#); [Li et al., 2015](#)). Crowd modelling involves simulating real-world crowds based on scientific hypotheses related to social, physical, biological and psychological factors ([Bel-lomo, Clarke, Gibelli, Townsend, & Vreugdenhil, 2016](#); [Hesham & Wainer, 2021](#); [Zhang et al., 2018](#)). For example, when looking at a crowd as a collective movement and studying its behaviour as a physical (e.g., fluid) or biological (e.g., animal swarm) phenomena including basic interactions, crowd models can describe real-world events using mathematical processes. Crowds can also be considered on a *macroscopic* (i.e., crowd) or *microscopic* (i.e., individual) level ([Kok, Lim, & Chan, 2016](#); [Zhang et al., 2018](#)). Macroscopic approaches simulate massive crowd movements in a way that considers a crowd to be a seamless, continuous flow without considering the interaction between individuals and is based on physical models, such as flowing fluid and continuum models. Such an approach is useful in evaluating large crowd characteristics including density, flow rate, size, and trends. Microscopic approaches, on the other hand, model individuals (pedestrians) as unique profiles in crowded situations using motion laws inspired by physical rules, e.g., cellular automata, social forces and psychological influences. By adopting the relevant crowd model, crowd simulation tools can generate various crowd scenarios and datasets in the form of text files, visual representations, graphical maps, image charts or tables ([Yang et al., 2020](#)). Many of these models have also been used in computer game engines including those generating crowd data (e.g. Grand Theft Auto V) ([Wang et al., 2019](#)).

Crowd simulators have been adopted extensively in practical applications such as pedestrian movement and crowd behaviour, crowd evacuation situations and environment layouts ([Abar, Theodoropoulos, Lemarinier, & O'Hare, 2017](#); [Caramuta et al., 2017](#); [Zhou, Dong, Ioannou, Zhao, & Wang, 2019](#)). Examples of these crowd simulation tools include *MassMotion* ([Oasys, 2019](#)), *SimWalk* ([Savannah Simulations, 2017](#)), *PedSim* ([Gloor, 2016](#)), *Legion* ([Still, 2000](#)), *Analogic* ([AnyLogic, 2014](#)), *NetLogo* ([Tisue & Wilensky, 2004](#)) and *Myriad* ([G.K. Still, 2004](#)). **MassMotion** developed and maintained by Oasys ([Kinsey, Walker, Swailes, & Butterworth, 2015](#)). MassMotion is an agent-based crowd simulation system implemented by two microscopic models: modified social force and least-effort model. **SimWalk** is an agent-based model simulation tool implemented by a social force and shortest-path model. A pedestrian database (measurement data) collected from real life is integrated with SimWalk to improve the results of the simulation ([SIMWALK, 1996](#)). **PedSim** is also an agent-based model that simulates pedestrian crowds and has been applied in different scientific projects representing bottlenecks and intersections. PedSim provides a library that can be used in other simulation tools, and an agent's behaviour can be extended. **Legion** is a pedestrian and crowd simulation tool which uses an agent-based model with 2D continuous space and 0.6 s time-steps ([Still, 2000](#)). It can handle various crowd scenarios with

different individual pedestrian behaviour by collecting data from many pedestrian types in different continents and contexts ([Caramuta et al., 2017](#)). Legion offers additional packages (e.g., Aimsun for Legion) to simulate scenarios such as traffic and vehicles and pedestrians while crossing a road ([Challenger, Clegg, Robinson, & Leigh, 2009](#)). **Anylogic** is one of the first multi-method simulation platforms that support macroscopic and microscopic simulation. Various industrial libraries such as pedestrian, road traffic and rail libraries enable its use in different applications ([Borshchev, 2013](#)). **NetLogo** is a platform that uses multi-agent models and is designed to model complex systems in which the crowd situation evolves. It was developed by (The Center for Connected Learning and Computer-Based Modeling) at Northwestern University in 1999. It has been used in different applications, including social and natural science, healthcare, business and traffic management ([Wilensky, 2012](#)). **Myriad** ([G.K. Still, 2004](#)) simulation environment can simultaneously model a variety of environments including network models, spatial models, and agent-based models making it possible to model a real-world setting. Myriad is especially helpful because it can identify when, where and how a system is likely to fail ([Dridi, 2015](#)). [Table 1](#) summaries the crowd simulation tools.

The GTA5 Crowd Counting (GCC) ([Wang et al., 2019](#)) and the AGORASET dataset ([Allain, Courty, & Corpetti, 2012](#)) are examples of publicly available synthetic crowd datasets. GCC is an example of a large-scale visual synthetic dataset used in crowd counting applications ([Wang et al., 2019](#)) and was generated using the well-known video game GTA5 (Grand Theft Auto 5). AGORASET is also a visual synthetic dataset for crowd video analysis ([Courty, Allain, Creusot, & Corpetti, 2014](#)). The simulated data represent a total of seven settings (corridor, single or multiple obstacles, escape, dispersion, Mekkah, sideway) and the method of simulation is based on Helbing et al.'s work on the social force model ([Helbing & Molnár, 1995a](#)) to retain realistic crowd behaviour, and Maya and Mental Ray renderer ([van der Steen & Boardman, 2012](#)) to reflect real footages. [Table 2](#) conducts a comparison between related

**Table 1**  
Examples of crowd simulation tools.

Name	Approach	Model	CAD (Y, N)	Visual	Accessibility/License
MassMotion ( <a href="#">Oasys, 2019</a> )	Micro	Social force, least-effort	Y	2,3-D	Closed source, commercial, but available with SDK for academic purposes.
SimWalk ( <a href="#">Savannah Simulations, 2017</a> )	Micro	Social force-shortest path	Y	2,3-D	Closed source, commercial
PedSim ( <a href="#">Gloor, 2016</a> )	Micro	Agent-based	N	2D	Open source, Free
Legion ( <a href="#">Still, 2000</a> )	Micro	Agent-based, Benefit cost	Y	2,3-D	Closed source, commercial
Anylogic ( <a href="#">AnyLogic, 2014</a> )	Macro and Micro	Agent-based, Discrete, system dynamics	Y	2,3-D	Closed source, Free version is available with limited features
NetLogon ( <a href="#">Tisue &amp; Wilensky, 2004</a> )	Micro	Spatial and Agent-based	N	2,3-D	Open source, Free
Myriad ( <a href="#">G.K. Still, 2004</a> )	Macro and Micro	Network, Spatial and Agent-based	Y	2,3-D	Closed source, commercial

CAD: (Y) the simulation tool allows to import the CAD drawing, (N) the simulation tool does not allow to import the CAD drawing.

**Table 2**  
A comparison between real and synthetic crowd datasets characteristics.

Dataset Reference	# Of Images, Scenes, Videos or Records	Type	Crowd Behaviour Analysis Goal											
			A	AD	P	CM	CO	G	L	S	SN	V		
UMN	3 scenes, 11 videos,	R, V		✓										
UCSD(UCSD, 2010)	PEDS1: 70, PEDS2: 28 videos	R, V		✓							✓			
UCSD (Chan et al., 2008)	2000 frames, 49,885 pedestrians	R, V						✓						
PETS (Ferryman & Shahrokni, 2009)	8 videos	R, V						✓	✓					
UCF (University of Central Florida. (2011a), 2011a)	Multiple	R, V	✓	✓	✓	✓	✓				✓	✓		
UCF-CC-50 (University of Central Florida. (2011a), 2011b)	50 images	R, V						✓						
HUER (Zawbaa & Aly, 2012)	Images and videos of six events	R, V	✓	✓	✓									
Mall (Chen et al.,2012)	2000 frames	R, V						✓						
Collective Motion (Zhou et al., 2013)	62 scenes, 413 videos	R, V				✓								
CUHK (Shao et al., 2014)	215 scenes, 474 videos	R, V				✓			✓					
Violent-Flows (Hassner et al., 2012)	246 videos	R, V				✓								
WWW (Shao et al., 2015)	94 Attributes, 8,257 scenes, 8 million frames 10,000 videos	R, V				✓	✓	✓				✓		
Shanghai Tech (Zhang et al., 2016)	Part A: 482, Part B:716	R, V						✓						
WorldExpo'10 (Zhang et al., 2016)	245 scenes, 2, 630 videos	R, V						✓						
Crowd-11(Dupont et al.,2017)	3,005 scenes, 6, 272 videos, 11 classes	R, V						✓	✓					
JHU-CROWD++ (Sindagi et al., 2020)	4, 372 images	R, V						✓						
NWPU-crowd (Wang et al., 2020)	5, 109 images	R, V						✓			✓			
CenceMe (Musolesi et al., 2008)	20 participants, 252 MB	R, N	✓											
Nodobo (Bell et al., 2011)	27 participants, 13, 035 Call records, 83, 542 message	R, N											✓	
D4D (Blondel et al., 2012)	500, 000 individual trajectories	R, N						✓	✓	✓				
The largest Swiss event (Blanke et al., 2014)	28,000 visitors	R, N						✓						✓
Non-visual crowd dataset (Irfan et al., 2018)	28 participants	R, N		✓									✓	
GCC (Wang et al., 2019)	15, 212 images, 7, 625, 843 person	S, V						✓						
AGORASET(Courty et al., 2014)	7 scenes	S, V						✓						
SIMCD	Four SIMCD datasets: Single Anomaly: 14, 068 records; Multiple Anomalies:12, 337 records; Prediction 1: 24, 123 records; Prediction 2: 24, 161 records	S, N		✓	✓									

“Type”: R- Real or S- Synthetic, V- Visual or N-Non-visual. “Goal”: A-Activity recognition; AD- Anomaly Detection; P- Prediction; CM- Crowd Collective Motion or Motion analysis; CO- Crowd Count or Density; G- Group Behaviour; L- Localisation or tracking; S-Segmentation; SG- Social network; V-Visualisation.

real and synthetic crowd datasets in the current crowd literature, including those proposed in this paper (SIMCD datasets). In contrast to the previous crowd datasets, the proposed SIMCD datasets are non-visual synthetic representations of crowd scenarios that can be used for creating crowd anomaly detection and prediction models. The proposed SIMCD datasets have been used for creating crowd anomaly detection models, using Hierarchical Temporal Memory (HTM), k-Nearest Neighbour (k-NN), Influence Outlierness (INFLO) and Local Outlier Probability (LoOP) (Bamaqa Sedky, Bosakowski, & Bastaki 2020), as well as for crowd prediction using HTM (Bamaqa et al., 2022).

#### 2.4. Discussion

Crowd datasets can be real or synthetic. The majority of the current real datasets are visual (i.e., video or image) using crowd monitoring systems. Most publicly available visual or non-visual crowd datasets, real or synthetic, have been used in counting tasks with few being used for crowd analysis (including anomalies). In addition, some of these datasets are designed to recognise individual human activities rather than the collective crowd behaviour. These findings motivate the generation of crowd anomaly detection data of the required scenarios. Generating real crowd anomaly detection datasets faces many challenges including difficulties in generating representative scenarios, due

to situational context and ethical concerns, and in terms of production complexity, cost and time; e.g., the pre-processing of visual data is time-consuming and requires expert annotation before being used. Synthetic alternatives would enable rapid generation of the synthetic datasets while overcoming challenges associated with their real counterparts. Crowd simulation tools offer flexibility in adjusting crowd scenarios and generating bespoke datasets that meet the specific crowd scenarios. The analysis of the current literature on crowd datasets supports previous reviews (Draghici & Steen, 2018; Haghani & Sarvi, 2018; Kaiser et al., 2018; Khan et al., 2020; Xie et al., 2020) which noted a lack of representative crowd anomaly detection datasets, either real or synthetic. MassMotion is a widely-used crowd simulator that can be used to generate synthetic crowd datasets with the required features. Therefore, this paper employs MassMotion to simulate crowd datasets that can be used for anomaly detection and prediction tasks.

#### 3. MassMotion for Crowd Simulation

Even though there are several crowd simulation tools, MassMotion is well suited to the task in hand; therefore this paper employs MassMotion to generate the required synthetic crowd datasets for prediction and anomaly detection tasks. The MassMotion software uses a micro-approach model to represent individual pedestrians in a crowd. By

simulating pedestrian movement, it facilitates knowledge about crowding, usage patterns, and occupant safety. It is widely used in industry and research for crowd simulation in the planning phase of a wide range of applications, such as railway terminals (Jin, Wang, Wang, Gu, & Wang, 2020), urban spaces, and large-scale events (e.g., Hajj event) and in crowd evacuation (Al-Ahmadi, Reza, Jamal, Alhalabi, & Assi, 2021). MassMotion can also incorporate aspects of crowd behaviour, such as lane formation and bottlenecks. Thousands of pedestrians' movements can be reliably simulated and the dataset can be exported in different formats (e.g., videos (mov, mp4, and wmv), images (png, jpg and tiff) or Comma-Separated Values (CSV)) (Oasys, 2019). The following list summarises the main reasons behind adopting MassMotion to generate the required synthetic crowd dataset.

- **Simulation Flexibility:** MassMotion can simulate various pedestrian activities in real-life scenarios by defining the simulation environment (e.g., stadiums, mass events, building evacuation, or railway terminals) and adjusting the agents (virtual pedestrians) with their activities. As an illustration, MassMotion can simulate buying a ticket in a rail station or fans' movements in a stadium.
- **Pedestrian intelligence:** In MassMotion, agents are aware of their surrounding environment and can adapt their speed and direction to reach and identify the target location, while dynamically responding to changes.
- **Scalability:** MassMotion is scalable and robust as it can simulate hundreds of thousands of pedestrians in a matter of hours (taking full advantage of multicore processors) making it valuable in simulating huge crowds.
- **2D and 3D compatibility:** MassMotion can handle 2D and 3D assets; it can import 2D Computer-Aided Design (CAD) files and develop them into 3D models.
- **Usability:** MassMotion has a straightforward and user-friendly Graphical User Interface (GUI), enabling rapid design and exploration without investing too much time or effort.
- **Extensibility:** MassMotion offers a software development kit (SDK) in different languages (e.g., C++, Java, Python and C#), enabling defining custom pedestrians' behaviour or connecting to other software tools through direct access to the MassMotion engine.
- **Reproducibility:** By reusing the same set of parameters and measurements of crowd scenarios for generating particular synthetic crowd datasets, MassMotion makes it easy to replicate these generated datasets for further evaluation or implementation purposes.

Using MassMotion makes it possible to design reliable scenarios representing pedestrians in mass gatherings which have been verified and validated with respect to real life settings. Kuligowski, Peacock, and Hoskins (2010) applied different validation and evaluation methods to the MassMotion simulator in comparison with other simulation models and pedestrian trials. A number of aspects were considered, including congestion associated with irregular flow resulting, for instance, from pedestrians moving against the general flow. It was observed that MassMotion represents the relationship between density and walking speed while the number of pedestrians in the trial area changes over time (O'Donnell, Roberts, & Debney, 2017). A distinction is also made between unidirectional and counter flow (Kinsey et al., 2015; Li, Wei, Kinsey, & Sun, 2018). MassMotion divides pedestrians' movement processes into two distinct tasks: agents' movements and navigation (Oasys, 2019). On the one hand, MassMotion uses a modified version of the microscopic social force model (Helbing & Molnár, 1995b) to estimate agents' movements and their responses to the environment. The social force model represents each agent (pedestrian) as an object affected by several forces, including impediments, goals, or adjoining forces (e.g., neighbours or obstacles). In addition, industry-standard guidelines have been developed by Fruin (Fruin, 1987) for general pedestrian planning to calibrate social forces in MassMotion (Oasys, 2019). Meanwhile, agent navigation decides the best route for the agent

to follow from the initial location. MassMotion uses the least-effort model for the best route selection, where the best path is the one with the lowest cost. The following Section describes in detail the entire workflow for generating a synthetic crowd dataset using the MassMotion simulator.

#### 4. SIMCD: SIMulated Crowd Data for Anomaly Detection and Prediction Generation Workflow

This Section demonstrates the entire workflow of using MassMotion to generate synthetic crowd datasets based on the specified crowd scenarios. Two proposed crowd scenarios are used to generate four different datasets that can be used for anomaly detection and prediction tasks. Fig. 2 exhibits the main steps for generating the synthetic datasets, which are: (1) scenario and model design, (2) crowd model simulation, (3) model verification, (4) dataset generation and (5) dataset pre-processing. The scenario and model design component involves preparation of crowd scenarios and anomaly context (e.g., specifying normal and abnormal events), scene creation (e.g., path, such as corridor, entrance and exit) and estimation of crowd parameters (e.g., number of agents and speed). Then, the crowd model simulation component creates the crowd model based on the specified scenario and the design parameters. The simulated crowd scenario is represented by a video that shows the pedestrians walking on the specified path towards their destination. The crowd model is validated and calibrated, any required changes being submitted back to the scenario and model design component to ensure more realistic outcomes that match the required scenario. The approved crowd model is then used for generating the dataset in the specified format. Finally, the dataset pre-processing component prepares the generated data for use in the prediction and anomaly detection tasks. The following subsections explain each component of the workflow in further detail.

##### 4.1. Scenario and Model Design

This Section outlines two crowd scenarios with different anomaly contexts for generating the synthetic datasets. The targeted synthetic crowd datasets are designed to exhibit anomalous behaviour based on crowd context and flow (e.g., irregular slowdown, unexpected increase in the density or unexpected direction). In these scenarios, high density and contra-flow travel represent crowd anomalies or abnormalities, which can be considered as warning signals of a critical situation. Therefore, the two designed crowd scenarios are (1) *Unidirectional with a single anomaly* (where high densities represent the anomaly) and (2) *Unidirectional with multiple anomalies* (where both high densities and people walking against the planned flow represent two types of anomalies). Both scenarios have been designed to evaluate the effectiveness of the anomaly detection and prediction crowd management models.

*Unidirectional with a single anomaly*, the first crowd scenario, simulates the crowd flow in a single direction. In this scenario, pedestrians move in one direction, straight from entrance A to exit B. The anomaly is represented by the density level, where low density is considered normal and high density is considered an anomaly. Normal moving density means that the number of pedestrians per square metre is less than four at any given time, while high moving density means there are four or more pedestrians per square metre (Smith, 1995; Still, 2011). Therefore, the scenario considers a density threshold of four pedestrians per square metre. In this first scenario, the crowd data represents pedestrians moving in normal densities (i.e., less than four) for almost 75% of the data size. In the single anomaly scenario, the number of pedestrians is gradually increased, from one person per square metre to two, and then three, for the first 75% of the simulation time. For the remaining 25% of the simulation time, the pedestrians move both in normal and high densities (four or higher, this being an anomaly) for some time before the density is reduced to normal levels (i.e., between 3 and 1).

Although density is a universally recognised critical condition of a

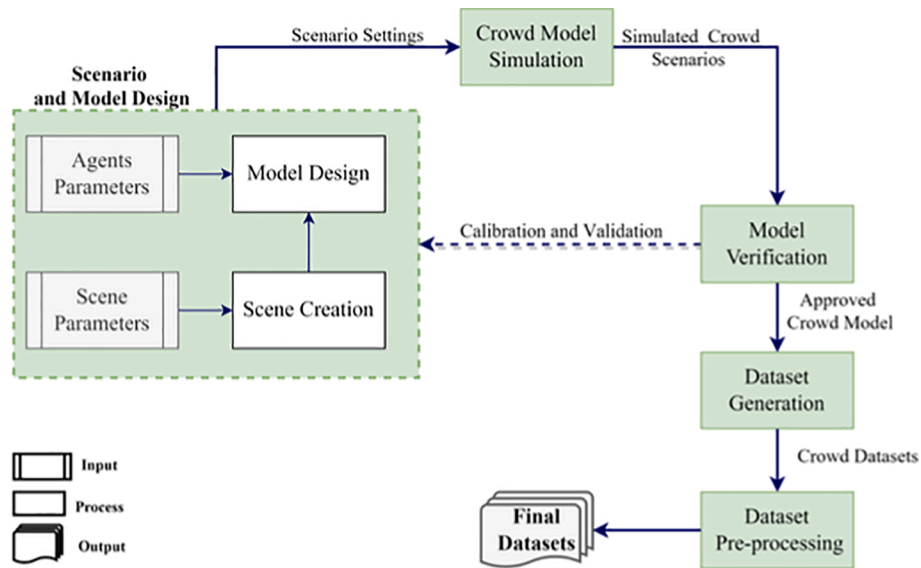


Fig. 2. Main Steps of the data generation process.

crowd situation, it may not be the only warning sign as densities in a critical situation may be similar to those under safe conditions (Feliciani & Nishinari, 2018). However, crowd flow (movement direction) is always considered to be an important indicator of a crowd’s critical condition. Therefore, the second scenario, *unidirectional with multiple anomalies*, considers both high densities and contra-flow as crowd anomalies. Initially, the pedestrians move in normal crowd densities and in the same, planned, walking direction. After that, the scenario shows pedestrians moving in high densities (i.e., four or more), while, at the same time, some move in the opposite direction. Finally, the scenario reduces densities to normal levels, while some people continue to move in the opposite direction to the planned flow. These two scenarios can be used as test cases for machine learning algorithms to detect abnormal behaviours resulting from high density spikes and movement in the opposite direction (Bamaqa et al., 2020).

4.1.1. Scene creation

Once the required crowd scenarios have been specified, the next step is to start the scene design in MassMotion. MassMotion provides flexible elements (e.g., floor, link, portals and barriers) to set up the required scene. The chosen design represents a corridor (represented by floor element) with single entrance and exit points (represented by portal element). The corridor is 20m by 5m giving an area of 100m<sup>2</sup>, as shown in Fig. 3. This scene design acts as the baseline that works for the previously described crowd scenarios, regardless of the density level, average speed and direction of the pedestrians.

4.1.2. Parameter estimation

The next step is careful estimation of the necessary parameters

required by the MassMotion engine to create the crowd simulation model and generate representative datasets for the previously described crowd scenarios. These parameters include agent’s (pedestrian’s) speed and number of agents (which defines the density level). These parameters can be estimated based on previous findings from the crowd literature, real datasets obtained from field observations or experts’ knowledge, as shown in Table 3. As an illustration, the default profiles of agents in MassMotion, such as agent speed, were estimated based on standard metrics and industry guidelines for general pedestrian characteristics, such as the work by Fruin (Fruin, 1987), and a variety of real datasets including evacuation and route choice surveys (Oasys, 2019). MassMotion gives the flexibility to customise the simulation properties (such as the profile values of agents), based on real cases or state-of-the-art domain knowledge, to achieve realistic representative crowd simulation. Besides, the speed rate can be set at the start of the simulation governed by choice of distribution (normal, constant, triangular, uniform, exponential or log-normal). From observations of real scenarios, the average normal walking speed can be estimated. This is adjustable according to demographical (e.g., gender, age and cultures) and geographical features (e.g., the environmental layout).

As can be seen in Table 3, observations of real walking behaviour are used to generate the proposed crowd datasets. In addition, Table 3 shows the normal and critical levels of crowd densities and demonstrates an inverse relationship between walking speed and crowd density. To simulate the specified scenarios, MassMotion requires input values for the minimum, maximum, and standard deviation of speed. Therefore, Table 4 has been created, based on values from Table 3, which shows normal (free, noncontact and average) and abnormal (contact, critical and crisis) cases of walking behaviour where pedestrians are split equally into healthy and weak individuals.

4.2. Crowd model simulation

After defining the crowd scenarios and specifying crowd parameters, this phase presents a simulation of the scene’s operations. MassMotion provides events such as journey, vehicle, timetable or evacuation, where each represents a different set of actions. The event type determines the scheduling involving the entry time of the agents and their tasks. The agents are created and positioned in the scene to do one or more tasks (e.g., moving to a destination or evacuating an area). For simulating the proposed scenarios, the journey event was chosen to determine a single-entry time for the agent and specify a single task to be executed. A single

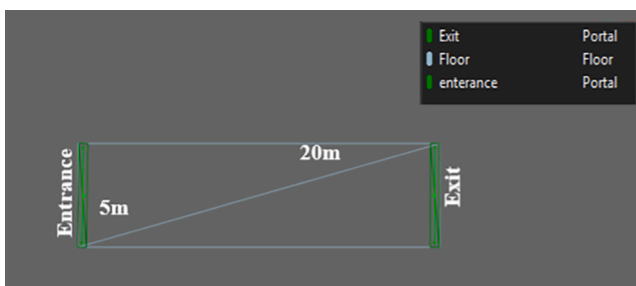


Fig. 3. Scenario design.

**Table 3**  
Relationship between walking speed, density and behaviour, adapted from (Ibrahim et al., 2016).

Scenario	Walking Behaviour	Density level	Density (Persons/m <sup>2</sup> )	Speed (m/s)	Reference
Planned path	Free Walking	Normal density	0.8	1.4	(Smith, 1995)
	Noncontact Walking	Normal density	1.8	0.8	(Smith, 1995)
	Semi-contact Walking	Normal density	2–3	0.6	(Helbing & Mukerji, 2012)
	Contact Walking	Start critical density (stagnation)	4	0.4	(Smith, 1995)
	Limited Walking	Critical density	5	n/a	(Oberhagemann, 2012)
		Possible crowd forces begin to occur		5.5	n/a

**Table 4**  
Crowd data conditions in normal and abnormal cases, including speeds and average densities.

State	Walking Behaviour	Density Persons/m <sup>2</sup>	Speed (m/s)			
			MIN	MEAN	MAX	STD
<b>Normal Cases</b>	Free – (Healthy pedestrian)	0.8	0.95	1.40	1.85	0.15
	Free – (Weak pedestrian)		0.55	1.00	1.45	0.15
	Non-contact – (Healthy pedestrian)	1.8	0.35	0.80	1.25	0.15
	Noncontact – (Weak pedestrian)		0.25	0.70	1.15	0.15
	Average – (Healthy pedestrian)	2.9	0.30	0.60	0.90	0.10
	Average – (Weak pedestrian)		0.15	0.45	0.75	0.10
<b>Abnormal cases</b>	Contact – (Healthy pedestrian)	4	0.25	0.40	0.55	0.05
	Contact – (Weak pedestrian)		0.15	0.30	0.45	0.05
	Critical – (Healthy pedestrian)	5	0.15	0.30	0.45	0.05
	Critical – (Weak pedestrian)		0.10	0.25	0.40	0.05
	Crowd Crisis – (Healthy pedestrian)	5.5	0.10	0.25	0.40	0.05
	Crowd Crisis – (Weak pedestrian)		0.07	0.22	0.37	0.05

journey corresponds to one case in walking behaviour in Table 4. Hence, in this work there is a need to determine more than one journey event (six journeys are assessed including healthy and weak pedestrians under normal conditions and another six journeys for abnormal situations) to simulate the proposed scenarios. Each journey requires the number of agents belonging to each walking behaviour category, their speed distribution and direction in order to populate the scene and the schedule time of active journeys to appear during specific times. For example, when the speed distribution was set (Mean = 1.4, Std = 0.15, Min = 0.95 and Max = 1.85) in the population's profile, as shown in Fig. 4, the journey required 5,770 agents during one hour to simulate the properties profile of Free- (healthy pedestrians) in the normal case and achieved an average density of 0.8 persons/m<sup>2</sup>. However, the number of agents to create walking behaviour in any given situation is not specified, as pedestrians adapt their walking behaviour with respect to the presence and direction of other agents and environmental components. To simulate the previously-described crowd scenarios, MassMotion requires parameters to be set for each journey event, such as the start time and duration, the population information (which determines the density parameter) and specification of entrance and exit points (which determine the direction), as shown in Fig. 4(a). The population information

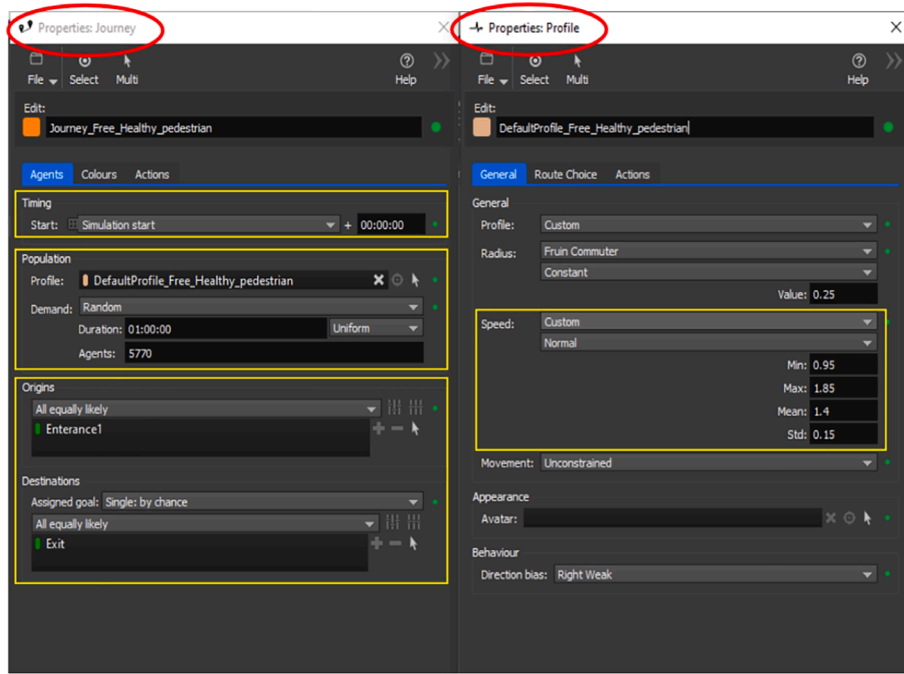
defines the agent's profile and the number of agents per journey. The agent's profile defines the physical (e.g., radius), behavioural (e.g., direction bias) and Speed (range of possible speed values based on normal distribution) properties for each agent, as shown in Fig. 4(b). The simulated crowd scenarios are then used to generate the corresponding crowd datasets with the inherent types of anomalies. Accordingly, a total of four crowd datasets have been created; two can be used for anomaly detection and the other two for prediction tasks, as described in Section 4.6.

#### 4.3. Crowd model verification

The verification has been conducted at two levels: (1) on the created crowd model and (2) on the generated datasets. The model creation is represented by a video generated by MassMotion which shows pedestrians walking along the specified path towards their destination. Fig. 5 presents the simulated crowd scenarios where pedestrians, identified by different colours, represent different walking behaviour in normal and abnormal cases. Fig. 5(a) represents the normal cases without high densities or counterflow. In contrast, Fig. 5(b) and (c) show the abnormal cases represented by counterflow and high densities, respectively. The video is used to validate the crowd model by comparing it against the pre-defined crowd scenario. For example, the average density and speed of individuals from random snapshots of the resulting video have been verified against the pre-defined design of the crowd scenario. In the case of any verification mismatch, the 'Scenario and Model Design' component is used to update the simulation parameters (such as the journey's start time, the number of agents, and their duration) to ensure more realistic outcomes that match the required scenario. Only when all criteria were satisfied was the model approved for subsequent dataset generation. The generated data have been also verified against the standard densities and speeds of the crowd cases, as shown in Table 4. For example, in the case of the normal density scenario, the density of the resulting dataset is always less than four; the borderline between normal and abnormal densities. Meanwhile, the validation ensures that the resulting density is equal to or greater than four in the case of abnormal densities. If the output of the simulation does not meet the standard, then the number of agents, their duration and the journey's start time are further tuned until the resulting density meets the requirements.

#### 4.4. Dataset generation

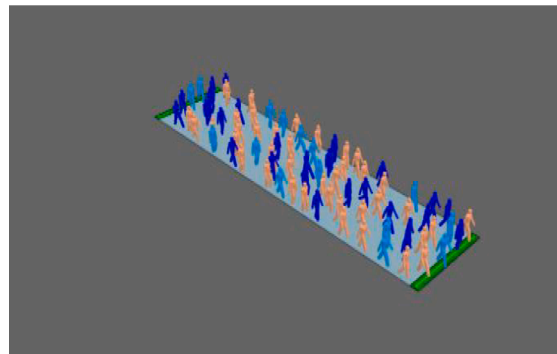
MassMotion exports the agents' physical attributes, such as Position, Speed, Heading (direction) and time, in different formats. Table 5 exhibits an excerpt from one of the synthetic crowd datasets that has been generated using MassMotion. The dataset has been exported to a CSV format and contains numerical information about the agent's position and movement attributes based on a sampling interval of one second. As shown in Table 5, the main features of the generated crowd dataset are the Frame number, Agent ID, Position (X, Y, and Z), Time, Speed, and Heading. The Speed feature refers to the distance (in metres) that the pedestrian covers per unit of time (each second). The Heading attribute represents the direction of the agent in degrees. As can be seen from Table 5, in each second, approximately five frames are being captured (i.



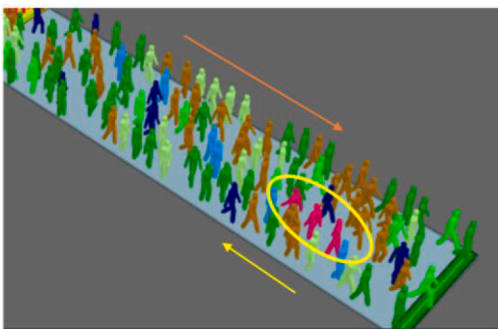
(a)

(b)

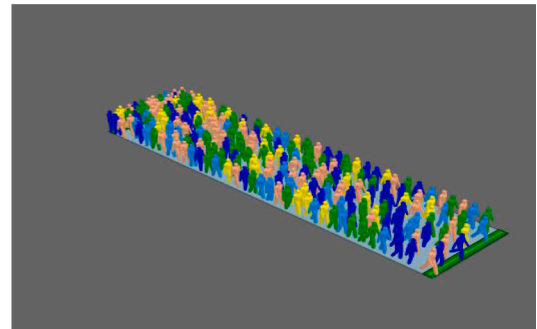
Fig. 4. (a) Journey properties; (b) Population profile of the free-healthy case.



(a) Unidirectional with normal density



(b) Unidirectional with opposite movement direction



(c) Unidirectional with high density

Fig. 5. Simulated crowd scenarios.

**Table 5**  
Original synthetic crowd dataset.

#Frame	Agent ID	X	Y	Z	Time	Speed (m/s)	Heading(Degree)
12	1001	1.31227	0	-13.6187	00:00:02	0.387138	-114.571
13	1001	1.27599	0	-13.4902	00:00:02	0.667857	-28.248
14	1001	1.24054	0	-13.3113	00:00:02	0.911904	-11.206
15	1001	1.2017	0	-13.093	00:00:03	1.10867	-10.089
16	1001	1.1733	0	-12.8428	00:00:03	1.25912	-6.476
13	1001	1.27599	0	-13.4902	00:00:02	0.667857	-28.248
14	1001	1.24054	0	-13.3113	00:00:02	0.911904	-11.206
15	1001	1.2017	0	-13.093	00:00:03	1.10867	-10.089
16	1001	1.1733	0	-12.8428	00:00:03	1.25912	-6.476
17	1001	1.14576	0	-12.5674	00:00:03	1.38362	-5.712
18	1001	1.13036	0	-12.2723	00:00:03	1.47775	-2.986
19	1001	1.12948	0	-11.962	00:00:03	1.55128	-0.162
20	1001	1.12912	0	-11.639	00:00:04	1.61523	-0.065
21	1001	1.11526	0	-11.307	00:00:04	1.66131	-2.391
22	1001	1.09854	0	-10.967	00:00:04	1.70219	-2.815
23	1001	1.08453	0	-10.6204	00:00:04	1.73447	-2.315
24	1001	1.08381	0	-10.2692	00:00:04	1.75565	-0.117
25	1001	1.08589	0	-9.91386	00:00:05	1.77683	0.334
26	1001	1.08381	0	-9.5552	00:00:05	1.79336	-0.331
27	1001	1.08163	0	-9.19383	00:00:05	1.80688	-0.346
28	1001	1.06394	0	-8.83198	00:00:05	1.81139	-2.800
29	1001	1.04657	0	-8.46817	00:00:05	1.82115	-2.733
30	1001	1.03287	0	-8.10272	00:00:06	1.82853	-2.146
30	1002	-3.11647	0	-13.6311	00:00:06	0.309808	132.180
31	1001	1.016	0	-7.73621	00:00:06	1.83447	-2.636
31	1002	-3.07604	0	-13.5292	00:00:06	0.548123	55.972

e., each agent often appears five times per second).

4.5. Data pre-processing

The main task of the data pre-processing phase is to make the data ready for machine learning models. The data pre-processing phase involves selecting relevant crowd features and pre-processing the dataset. The generated dataset represents individual pedestrians (agents); however, this approach is concerned with the crowd level itself (e.g., how many pedestrians are in a specific area at any point in time) to provide information describing global parameters such as density and to understand the crowd state at different times. Therefore, the data pre-processing focuses on performing aggregated statistical calculations to compute the average values of the essential features, such as Speed and Heading. The step also calculates new features based on existing ones, as shown in Table 6. As an illustration, columns of interest (such as Speed and Heading of individuals) have been selected, and average values have been calculated. The Heading column has been modified; for example, by converting negative values to positive by adding 360° to the original heading value. The rationale of modifying the “Heading” column is to meet the need for a positive aggregated value for each individual; so that, when the average is calculated, the normal range can be distinguished easily from an abnormal range of degrees. For example, in this context, the normal average Heading is within the range from 80° to 93°; hence, positive values are used, so any value higher than 93° is considered an anomaly. Finally, new columns have been added (e.g., Agent Count, Density, Level of Crowdedness, Severity Level). The Agent Count column, in Table 6, represents the number of pedestrians in a predefined area at every second. The Density column represents the number of pedestrians per square metre in a predefined area in one second, where the area in this design equals 100 m².

The newly estimated Level of Crowdedness and the Severity Level columns enable a threshold to be set for congestion under safe conditions to estimate the regularity of crowd movements and identify any abnormal situations, as shown in Tables 7 and 8. The Level of Crowdedness column represents five levels based on Density definitions in the literature, where the crowd movement is considered normal if the level of crowdedness is less than four, otherwise, it is abnormal. Multi-directional movement is more critical than unidirectional for given

**Table 6**  
Pre-processed SIMCD.

Speed m/s	Heading Degree	Agent Count	Density Persons/m²	Level of Crowdedness	Severity Level
1.1339	88.3671	76	0.76	1	0
1.1499	89.2521	88	0.88	1	0
1.1406	89.5428	90	0.9	1	0
1.1499	89.2521	88	0.88	1	0
0.7264	89.2905	177	1.77	1	0
0.7145	89.8208	180	1.8	2	0
0.6954	89.7852	182	1.82	2	0
0.7128	89.4686	185	1.85	2	0
0.6371	88.6367	200	2	2	0
0.6252	89.7749	201	2.01	3	0
0.6339	89.0087	204	2.04	3	0
0.508	89.1085	228	2.88	3	0
0.4856	88.2756	287	2.87	3	0
0.4832	88.7977	293	2.93	3	0
0.4861	88.3205	292	2.92	3	0
0.4023	87.9308	389	3.89	3	0
0.409	87.6874	393	3.93	3	0
0.3876	86.8984	402	4.02	4	2
0.391	86.4752	407	4.07	4	2
0.3854	87.2882	409	4.09	4	2
0.3858	88.5148	410	4.1	4	2
0.3413	87.0731	489	4.89	4	2
0.3476	86.4039	494	4.94	5	2
0.3519	86.1051	496	4.96	5	2
0.3534	86.9419	498	4.98	5	2
0.3342	87.3765	496	4.96	5	2
0.8317	98.9525	175	1.75	1	1
0.8099	101.0435	175	1.75	1	1
0.7496	100.9884	177	1.77	1	1
0.7488	101.67	181	1.81	2	1
0.7413	101.2632	184	1.84	2	1
0.7097	99.4066	187	1.87	2	1
0.2912	96.7623	390	3.9	3	1
0.2903	98.3493	393	3.93	3	1
0.2855	100.0678	396	3.96	3	1
0.2788	100.9259	399	3.99	3	1
0.2834	101.3003	401	4.01	4	3
0.2894	99.8226	403	4.03	4	3
0.2841	98.9516	404	4.04	4	3
0.2917	98.0279	409	4.09	4	3

**Table 7**

Crowd state based on Level of crowdedness.

Density Persons/m <sup>2</sup>	Crowd behaviour state	Level of Crowdedness
Less than 1.79	Normal Cases	Free walk 1
Between 1.79 and 2		Non-contact 2
Between 2 and 3.99	Abnormal Cases	Average 3
Between 4 and 4.99		Contact 4
5 and above		Critical 5

**Table 8**

Crowd state based on severity levels.

Density Persons/m <sup>2</sup>	Heading State	Crowd behaviour state	Level of crowdedness	Severity level
Less than 4	Planned	Normal Cases	1, 2 or 3	0
4 and more		Abnormal	4 or 5	2
Less than 4	Opposite	Cases	1,2 or 3	1
4 and more			4 or 5	3

density levels. Therefore, the new Severity Level column is proposed as an estimate based on Density and Heading (direction) to measure these characteristics and obtain an entire picture of serious crowd situations. This work employs four severity levels based on Heading and Density, (Table 8). Ranging from zero, meaning no risk (i.e., representing a normal crowd state where there is no high crowd density and people are moving in a planned direction), to level three.

- Level 1 represents the opposite direction with normal densities (i.e., densities vary between 1 and 3 agents per square metre).
- Level 2 represents the planned direction with high densities (i.e., densities include 4 or more of agents per square of metre).
- Level 3 represents the critical, abnormal state (high densities with movement in opposite direction).

Both the Level of Crowdedness and Severity Level columns represent the ground truth (i.e., labels) for the generated dataset and may assist in devising proactive anomalies and prediction models to detect anomalies and achieve efficient crowd management. The generated dataset is publicly available.

4.6. Exploratory data analysis

This Section demonstrates a quick overview of both statistical and visual exploratory data analysis of the pre-processed crowd dataset. In Section 4.1, this paper considers two different crowd scenarios; unidirectional with a single anomaly and unidirectional with multiple anomalies. Fig. 6 exhibits the behaviour in a unidirectional scenario with a single anomaly, where the anomaly is represented by high-

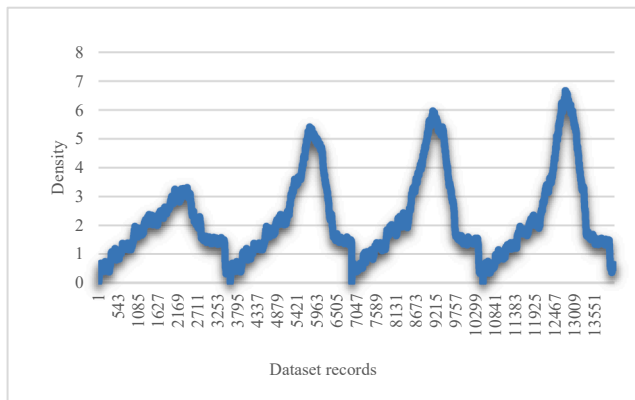


Fig. 6. Unidirectional with a single anomaly (high density) scenario.

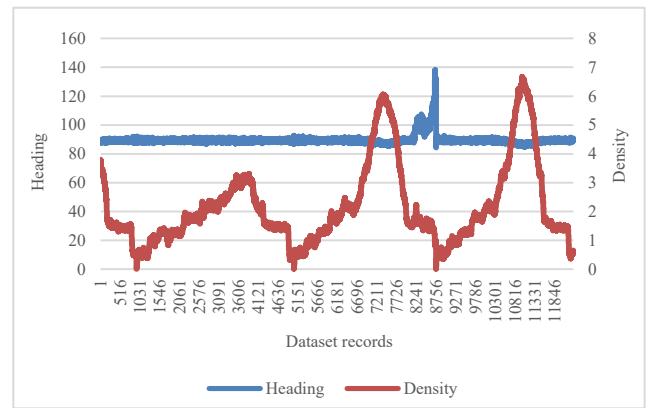


Fig. 7. Unidirectional with multiple anomalies (high density and opposite direction) scenario.

density values (equal or higher than four). The second scenario, unidirectional with multiple anomalies, exhibits two anomalies resulting from the high density and agents walking in the opposite direction (Heading), as shown in Fig. 7. Based on the proposed scenarios, four simulated crowd datasets have been aggregated to meet anomaly detection and prediction requirements. The description of the simulated crowd datasets, including SIMCD-Single Anomaly, SIMCD-Multiple Anomalies, SIMCD-Prediction 1 and SIMCD-Prediction 2 are presented in the following two subsections.

4.6.1. SIMCD-anomaly datasets

The SIMCD-anomaly datasets are represented by the SIMCD-Single Anomaly and SIMCD-Multiple Anomalies datasets. The SIMCD-Single Anomaly dataset contains crowd data representing the unidirectional flow scenario with high density regarded as a single anomaly. The data has 14,068 records. Each record has an integer label for the Level of crowdedness where (1, 2 or 3) represents normal cases and (4 or 5) represents anomalies, as shown in Table 5. This data was prepared to serve for crowd anomaly detection applications. Being data created for training the anomaly detector, the first 80% of the generated data represents normal crowd densities. The remaining 20% of the generated data includes both normal and abnormal classes, see Fig. 6.

On the other hand, the SIMCD-Multiple Anomalies dataset exhibits two types of anomalies (which are, high density and opposite direction). This dataset includes a sequence of events starting with the unidirectional flow with normal crowd densities (Level of crowdedness < 4), followed by a crowd density that has a sudden surge, representing an anomalous behaviour. Finally, the crowd density returns to normal. However, while the Level of densities is normal, a group of pedestrians emerges from the opposite direction. The data has 12,337 records.

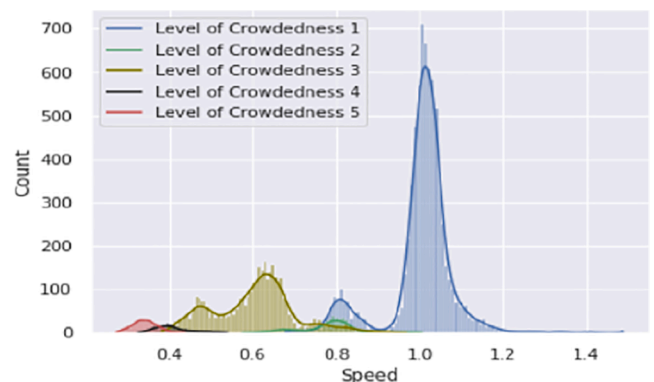


Fig. 8. SIMCD-anomaly detection speed distribution.

Eighty percent (80%) of the data from the beginning is used for training and contains only normal cases, see Fig. 7.

Fig. 8 shows the Speed distribution of SIMCD-anomaly detection datasets for each level of crowdedness. As can be seen in Fig. 8, the majority of data represents normal levels of crowdedness (levels 1 to 3; the blue, green and olive curves). However, the crowd anomalies are represented by two levels of crowdedness (levels 4 and 5; the black and red curves). Only small portion of the data represents crowd anomalies, which is somewhat similar to the proportion of anomalies in real-life scenarios.

#### 4.6.2. SIMCD-prediction

The SIMCD-prediction datasets are based on the SIMCD-Prediction 1 and 2 datasets. The SIMCD-Prediction 1 dataset contains crowd data with normal and abnormal cases, including two types of anomalies (high crowd density and a flow opposite to the planned direction). The Severity Level column is added to this data which is calculated based on crowd densities and headings (direction) and includes four levels of severity, as shown in Table 8. This column serves as the ground truth for prediction models. The data size equals 24,123 records which include 19,000 training records and 5,123 testing records. Some details of SIMCD-Prediction 1 are presented in Table 9 and Fig. 9. Table 9 summaries statistics of the preprocessed crowd dataset (SIMCD-Prediction 1) by showing the number of samples (count), mean, maximum and minimum values of the selected features. For example, the SIMCD-Prediction 1 consists of 24,123 aggregated observations with an average speed of 0.74 m/s.

The heatmap in Fig. 9(a) shows an inverse relationship between crowd Speed and Density, which can be seen from the strong negative correlation between the two features. Fig. 9(b) shows the relationship between the Speed, Heading, Density and Level of crowdedness in relation to the Severity Level of the crowd. As an illustration, normal speeds (which reflect normal densities), while walking in the planned direction result in a Severity Level of zero. However, walking in the opposite direction, regardless of the speed, will always result in an abnormal severity level, as in level 1 and 3. Slow speeds usually result in high densities and an abnormal severity level, as in level 2 and 3. Finally, regardless of direction, Fig. 9(b) shows that levels 1, 2 and 3 in the level of crowdedness reflect normal densities, and are equivalent to Severity Levels 0 and 1. Moreover, the levels of crowdedness 4 and 5 reflect abnormal densities and, are equivalent to severity levels 2 and 3.

In addition, the SIMCD-Prediction 2 dataset consists of the same training dataset presented in SIMCD-Prediction 1, in addition to new testing data. The test data of the SIMCD-Prediction 2 dataset includes different orders of severity levels than those used in the training phase to make testing data more realistic and to evaluate how machine learning models adapt to changes in the dataset. Fig. 10 summarises the features of the synthesised SIMCD-Prediction 2 dataset, which consists of 24,161 records. Fig. 11 shows the distribution of Speed (a), Density (b) and Heading (c) for each class of crowd severity level using the SIMCD-Prediction 2 dataset. The blue curves in Fig. 11(a)–(c) represent Severity Level 0, reflecting normal walking speeds (0.4 to 1.4 m/s), normal densities (i.e. less than four persons) and normal heading (the planned walking direction). The green curves represent Severity Level of

class 1, clearly reflecting the situation where normal speeds and densities co-exist with opposite walking direction (more than normal pre-defined degrees). The black curves represent Severity Level of class 2 indicating low-speed levels with high densities while heading distribution is normal. Finally, Severity Level 3 is represented by the red curves which show the worst-case scenario including low speed levels, high level of densities and opposite heading.

## 5. Experimental results

This section shows the performance evaluation of the crowd anomaly detection and prediction tasks using the synthetically generated SIMCD-anomaly detection and prediction datasets, as presented in the next two subsections.

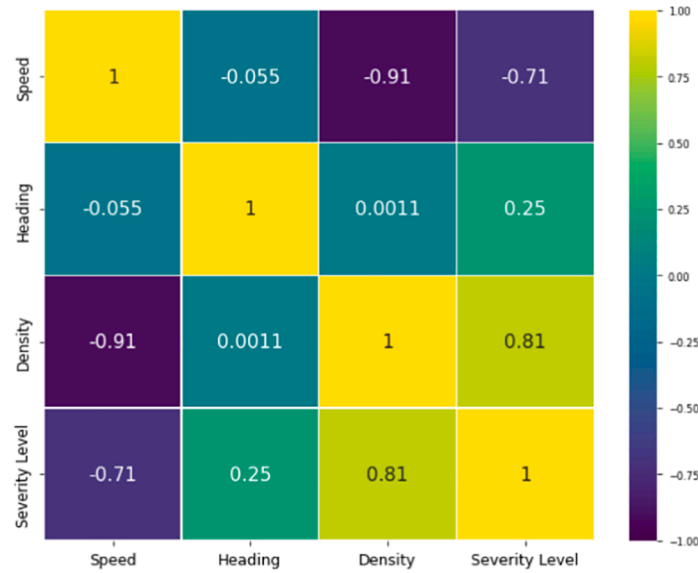
### 5.1. Anomaly detection experiments

Considering the crowd anomaly detection problem, the data is expected to have significant class imbalance as the percentage of abnormal cases is usually far lower than the normal counterparts. The abnormal data do not explicitly show up in the training dataset during the training phase, but are more likely to appear in the testing phase. The model's objective is to learn the normal patterns of the data during the training phase and distinguish this behaviour from any anomalous patterns occurring during the testing phase. Therefore, a hold-out validation technique is followed to split the data into training (80%) and testing (20%). Accordingly, the generated synthetic crowd dataset is initially designed to cover the normal cases in the first 80% of the entire dataset size. In this probationary period, the result of the model is not scored, but the model trains for the given patterns. The remaining 20% of the crowd dataset includes both normal and abnormal cases, and this will be used for testing and evaluation in the various experiments.

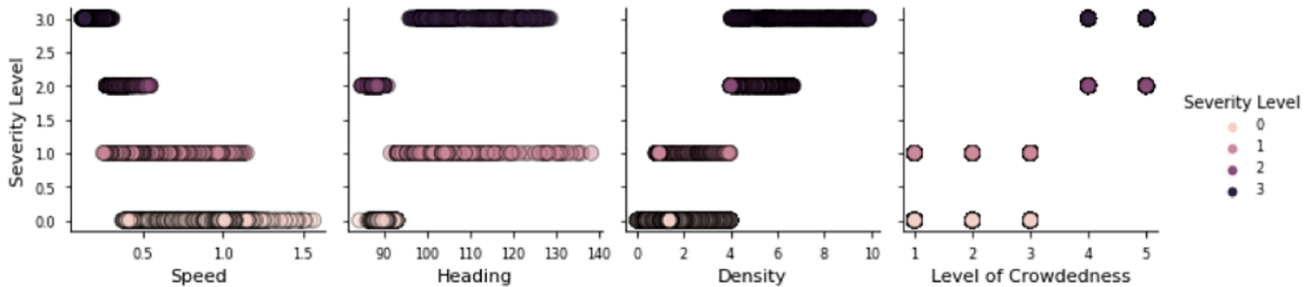
Fig. 12 shows the block diagram for the crowd anomaly detection experiments. Crowd data containing single or multiple anomalies (SIMCD-Single Anomaly and SIMCD-Multiple Anomalies) are used as inputs for evaluating various crowd anomaly detection models. The conducted anomaly detection experiments evaluate four anomaly detection models, which are: Cortical Learning Algorithms based on the Hierarchical Temporal Memory (CLA-based HTM), k-Nearest Neighbour Global Anomaly Score (k-NN-GAS), Local Outlier Probability (LoOP) and the Influence Outlier (IO). The CLA-based HTM is an online and unsupervised biological anomaly detector that computes anomalies in streaming data (Hawkins, 2014). The CLA-based HTM uses various encoders, such as Scalar and Coordinate, for encoding the input data (Purdy, 2016). The scalar encoder encodes numerical data into the equivalent Sparse Distributed Representation (SDR), and requires specifying the minimum and maximum values for each feature (e.g., Speed and Heading). The coordinate encoder uses a 3D integer coordinate space, and was achieved by substituting the X and Y coordinates with Heading and Speed features of the crowd dataset and replacing the radius with the Density. However, k-NN-GAS, LoOP and IO are unsupervised statistical Nearest Neighbour based anomaly detectors. The k-NN-GAS calculates a global anomaly score based on the average distance to the k-Nearest Neighbours (Angiulli & Pizzuti, 2002). However, LoOP

**Table 9**  
Summarised statistics of SIMCD-Prediction 1.

	Speed m/s	Heading Degree	Agent Count	Density Persons/m <sup>2</sup>	Level of Crowdedness	Severity Level
Count	24,123	24,123	24,123	24,123	24,123	24,123
Mean	0.74	90.31	251.09	2.51	2.34	0.51
Std	0.28	4.80	167.62	1.68	1.46	0.86
Min	0.12	84.32	1.00	0.01	1.00	0.00
25%	0.50	88.48	134.00	1.34	1.00	0.00
50%	0.78	89.17	187.00	1.87	2.00	0.00
75%	1.01	89.80	336.00	3.36	3.00	1.00
Max	1.57	138.16	990.00	9.90	5.00	3.00



(a)



(b)

Fig. 9. Relationships among different features of the SIMCD-Prediction 1.

and IO are local density-based anomaly detectors that estimate an anomaly score representing the probability of a datapoint as being an outlier/anomaly (Jin, Tung, Han, & Wang, 2006; Kriegel, Kröger, Schubert, & Zimek, 2009). The LoOP makes use of the Independent Component Analysis (ICA), which is a dimensionality reduction technique that depends on array processing and data analysis to recover the unobserved data samples from the oversampled dataset (Krithigarani & Karthik, 2014). In addition, the IO makes use of the Singular Value Decomposition (SVD), which is a common method that is used in matrix decomposition. In the SVD-IO the decomposed lower dimensional features are used for anomaly detection with influences an outlier module (Kumar & Nasser, 2012). The adopted anomaly detection models output anomaly scores (reflecting the status of the target label ‘Level of Crowdedness’) for each input data record. This process is completely unsupervised and the label in the dataset is used only for testing and evaluation purposes. The anomaly detection models output an anomaly score which, when normalised if necessary, gives a number between 0.0 and 1.0. Moreover, there is a need to identify the optimum threshold for anomaly score that distinguishes the crowd anomalies from normal cases. Based on the selected anomaly threshold, anomalies will be identified and the model’s performance is estimated by calculating the performance metrics (Accuracy and F-score).

5.1.1. Single anomaly detection

Fig. 13 shows the performance of the CLA-based HTM, using both scalar and coordinate encoders, k-NN-GAS, ICA-LoOP and SVD-IO in detecting crowd anomalies; using SIMCD-Single Anomaly dataset. It is

apparent that both versions (Scalar and Coordinate) of the CLA model significantly outperform their counterparts for detecting single anomalies. For example, CLA with Coordinate encoder improved the performance by around 13% compared to KNN-GAS, ICA-LoOP and SVD-IO. Moreover, the Coordinate encoder outperforms the Scalar one by around 7%.

5.1.2. Multiple anomalies detection

This experiment uses the SIMCD-Multiple Anomalies dataset to evaluate the performance of the CLA-based HTM, k-NN-GAS, ICA-LoOP and SVD-IO. Fig. 14 confirms the results found in Fig. 13, in the previous experiment, where the CLA models (using Scalar or Coordinate encoders) significantly outperform other anomaly detection counterparts. The CLA with the Coordinate encoder improved the performance by around 18% F-score compared to the kNN-GAS, ICA-LoOP and SVD-IO.

5.2. Prediction experiments

The crowd prediction experiments aim to predict a sequence of crowd severity levels; predicting 60 steps ahead. Fig. 15 shows the block diagram for the crowd prediction experiments. The experiments evaluate several sequence prediction models, CLA-based HTM and encoder-decoder Long Short-Term Memory (LSTM)-based models e.g., LSTM-LSTM, Convolutional Neural Network (CNN)-LSTM and ConvLSTM, using the SIMCD-Prediction 1 dataset. LSTM offers the ability for long-term dependencies to be modelled by means of gating mechanisms (Hochreiter & Schmidhuber, 1997). A CNN is another class of artificial

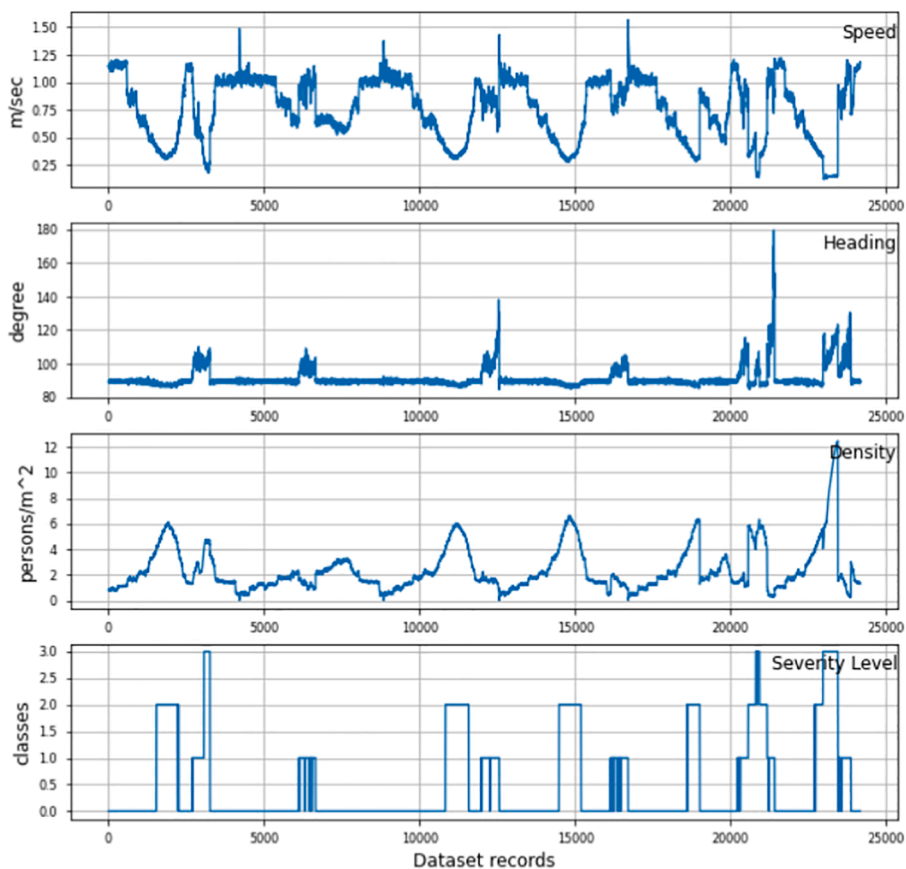


Fig. 10. Summarised visualisations of all features of the SIMCD-Prediction 2.

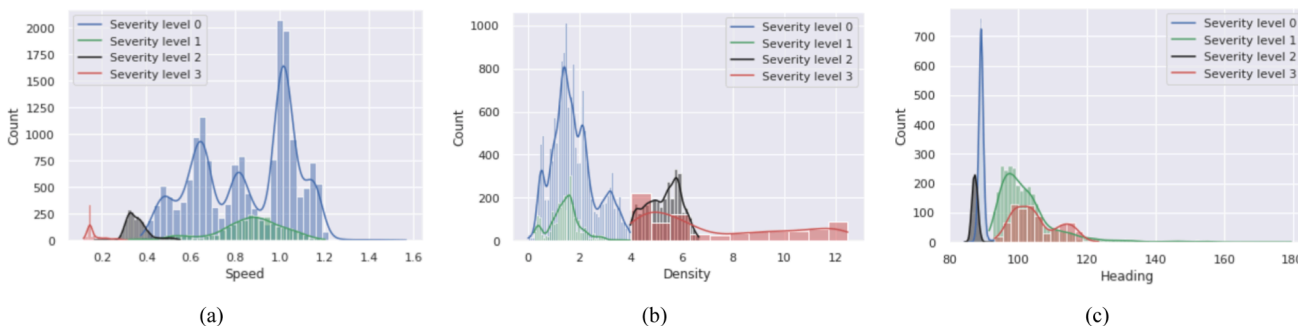


Fig. 11. Distribution of Speed, Heading and Density for each class of crowd severity levels using SIMCD-Prediction 2.

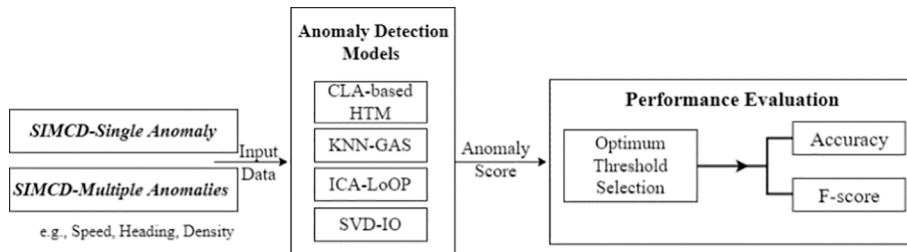


Fig. 12. The experimental design for crowd anomaly detection.

neural networks that handles two-dimensional image data and can capture spatial properties of images and videos (LeCun et al., 1998). LSTM-LSTM architecture uses an LSTM network to act as an encoder and a decoder. CNN-LSTM architecture uses CNN network as an encoder for

processing the sequence-based input, while LSTM acts as the decoder for CNN’s output. ConvLSTM uses convolutions of the input sequence to feed data into the encoder LSTM cells, which is different from using a complete CNN for the encoder. The LSTM-LSTM experiments have been

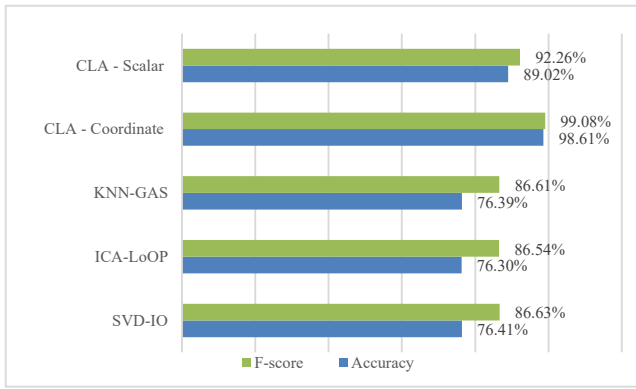


Fig. 13. CLA versus k-NN-GAS, ICA-LoOP and SVD-IO for detecting anomalies using SIMCD-Single Anomaly dataset.

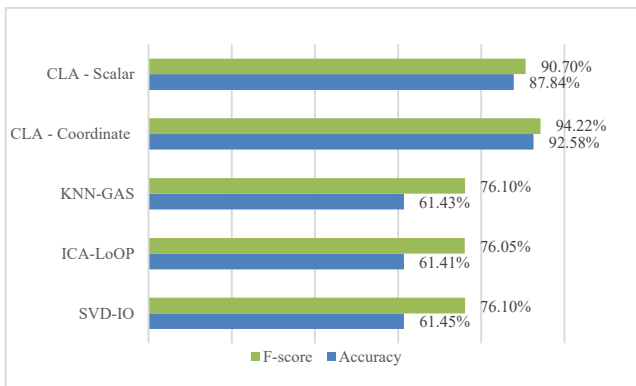


Fig. 14. CLA versus k-NN-GAS, ICA-LoOP and SVD-IO for detecting anomalies using SIMCD-Multiple Anomalies dataset.

conducted using *online* (to compare the results with the online CLA-based HTM) and *offline* modes. The online LSTM mode describes the case when the batch size is set to one, while in the offline LSTM, the batch size is greater than one and less than the size of the training dataset; a batch size of 20 has been used in the experiments. For the prediction model, the evaluation process follows the same procedure with data split between training and testing. Finally, the Accuracy and F-score metrics of the last item in a predicted sequence are used to evaluate the performance of the used prediction models.

Fig. 16 shows the performance of the conducted crowd prediction experiments. By and large, the offline LSTM-based models outperform the online ones. The offline batch-based learning models using encoder-decoder LSTM-LSTM and ConvLSTM achieve higher F-score than the online CLA-based HTM. As can be seen in Fig. 16, the encoder-decoder LSTM-LSTM has achieved an F-score of 93.85%, ConvLSTM has achieved 94.07%, whereas the CLA-based HTM has scored 91.28%. In addition, the CLA-based HTM and CNN-LSTM demonstrate comparable

performance, around 91% F-score; however, the CLA-based HTM model supports online learning.

### 6. Conclusion

Crowd datasets and specific crowd features originate either from real observations (natural setting or experiment) or by generating synthetic datasets. Several crowd management applications have used these datasets, including crowd anomaly detection, predictions, and activity analysis classification. The current study presented SIMulated Crowd Datasets (SIMCD) to be used for the development of crowd anomaly detection and prediction models. The MassMotion crowd simulation tool was employed to generate the developed datasets, where two crowd scenarios were simulated to allow study of their behaviour and anomalies. These crowd scenarios form the basis for identifying the main crowd features and generating the required synthetic crowd datasets. The simulated scenarios represent two anomalies: unidirectional with a Density-based single anomaly and unidirectional with Density- and Heading-based multiple anomalies. The paper demonstrated the workflow for generating the synthetic datasets, which consists of five main steps: (1) scenario and model design, (2) crowd model simulation, (3) model verification, (4) dataset generation and (5) dataset pre-processing. The generated data has been prepared by adding new features such as density, level of crowdedness, and severity levels. The average density of pedestrians has set the level of crowdedness column: five classes, normal and abnormal events have been factored in. Moreover, the severity level, tied to density and heading, has also been identified. The paper introduced these features as ground truth for crowd anomaly detection and prediction datasets. The synthetically generated crowd dataset, SIMCD, would facilitate the development of crowd learning models; primarily to enable innovative models to be trained, tested, validated, and evaluated.

As a future work suggestion, once we have access to real crowd data for the required scenario, we will focus on evaluating the performance of different anomaly detection models using both the real and the synthetic

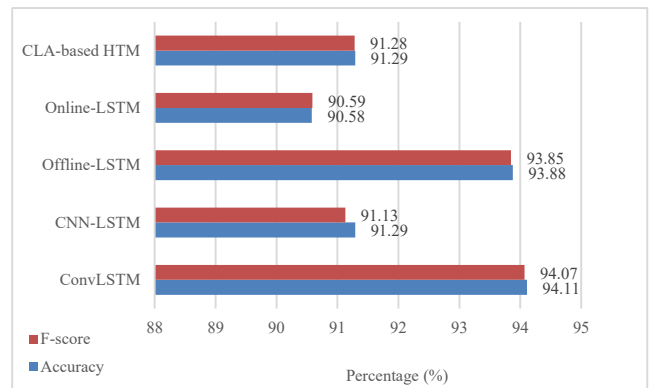


Fig. 16. CLA-based HTM, Encoder-Decoder LSTM, CNN-LSTM and ConvLSTM for crowd severity prediction using SIMCD-Prediction 1.

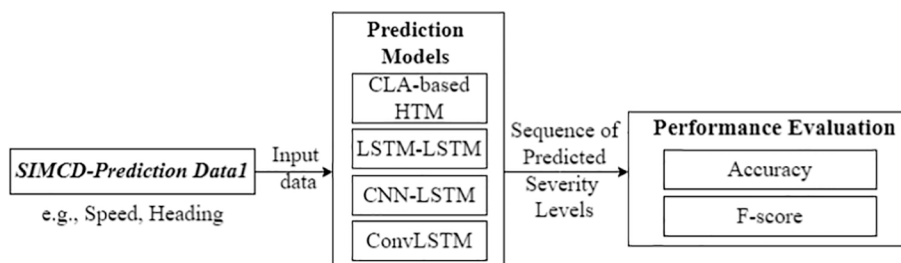


Fig. 15. The experimental design for crowd prediction.

data that have been proposed in this paper. In addition, we will consider developing an online repository of both real and synthetic crowd datasets which would be of paramount importance. This online repository should provide easy access and a proper search mechanism for the crowd datasets. To create this repository, various subtasks need to be investigated, such as (1) Designing a confined structure for both real and synthetic crowd datasets with proper use of *meta*-information to facilitate the search functionality of these datasets, (2) Generating various synthetic crowd datasets that cover the critical scenarios for anomaly detection tasks, and (3) Applying generic pre-processing and data wrangling tasks as well as video analysis on existing visual real crowd datasets, so that they can be stored in the chosen confined structure. A carefully built online repository of crowd datasets would allow future crowd management research to proceed with more robust and realistic datasets.

### Declaration of Competing Interest

The authors declare that they have no known competing financial interests or personal relationships that could have appeared to influence the work reported in this paper.

### Acknowledgements

Amna Bamaqa is carrying out her PhD studies at Staffordshire University. Amna acknowledges Taibah University and the Ministry of Education in Saudi Arabia for funding and supporting her PhD project.

### Appendix A. Supplementary data

Supplementary data to this article can be found online at <https://doi.org/10.1016/j.eswa.2022.117475>.

### References

- Abar, S., Theodoropoulos, G. K., Lemarini, P., & O'Hare, G. M. P. (2017). Agent based modelling and Simulation tools: A review of the state-of-art software. *Computer Science Review*. <https://doi.org/10.1016/j.cosrev.2017.03.001>
- Abuarafah, A. G., Khoziem, M. O., & AbdRabou, E. (2012). Real-time crowd monitoring using infrared thermal video sequences. Retrieved from *Journal of American Science*, 8(3), 133–140 [https://www.academia.edu/download/69244655/015\\_8123am0803\\_133\\_140.pdf](https://www.academia.edu/download/69244655/015_8123am0803_133_140.pdf).
- Al-Ahmadi, H. M., Reza, I., Jamal, A., Alhalabi, W. S., & Assi, K. J. (2021). Preparedness for mass gatherings: A simulation-based framework for flow control and management using crowd monitoring data. *Arabian Journal for Science and Engineering*, 46(5), 4985–4997. <https://doi.org/10.1007/s13369-020-05322-8>
- Allain, P., Courty, N., & Corpetti, T. (2012). AGORASET: A dataset for crowd video analysis. In *In 1st ICPR international workshop on pattern recognition and crowd analysis* (pp. 1–6).
- Amirian, J., Hayet, J. B., van Toll, W., & Pettré, J. (2019). Data-Driven Crowd Simulation with Generative Adversarial Networks. *ArXiv*. ACM. <https://doi.org/10.1145/3328756>.
- Angiulli, F., & Pizzuti, C. (2002). Fast outlier detection in high dimensional spaces. In *Lecture Notes in Computer Science (including subseries Lecture Notes in Artificial Intelligence and Lecture Notes in Bioinformatics)* (Vol. 2431 LNAI, pp. 15–27). Springer Verlag. [https://doi.org/10.1007/3-540-45681-3\\_2](https://doi.org/10.1007/3-540-45681-3_2).
- AnyLogic. (2014). AnyLogic: Simulation Modeling Software Tools & Solutions for Business. Retrieved January 9, 2022, from <https://www.anylogic.com/>.
- Assem, H., & Osullivan, D. (2017). RCMC: Recognizing Crowd-Mobility Patterns in Cities Based on Location Based Social Networks Data. *ACM Trans. Intell. Syst. Technol. Article ACM Transactions on Intelligent Systems and Technology*, 8(70). <https://doi.org/10.1145/3086636>
- Bamaqa, A., Sedky, M., & Bastaki, B. B. (2022). Reactive and proactive anomaly detection in crowd management using hierarchical temporal memory. *International Journal of Machine Learning and Computing*, 12(1). <https://doi.org/10.18178/ijmlc.2022.12.1.1072>
- Bamaqa, A., Sedky, M., Bosakowski, T., & Bastaki, B. B. (2020). Anomaly Detection Using Hierarchical Temporal Memory (HTM) in Crowd Management. In *Proceedings of the 2020 4th International Conference on Cloud and Big Data Computing* (Vol. 353270, pp. 37–42). 10.1145/3416921.3416940.
- BBC. (2015, September 24). Hajj stampede: At least 717 killed in Saudi Arabia - BBC News. Retrieved February 5, 2021, from <https://www.bbc.co.uk/news/world-middle-east-34346449>.
- Bell, S., McDiarmid, A., & Irvine, J. (2011). Nodobo: Mobile Phone as a Software Sensor for Social Network Research. In *2011 IEEE 73rd Vehicular Technology Conference (VTC Spring)* (pp. 1–5). IEEE. 10.1109/VETECS.2011.5956319.
- Bellomo, N., Clarke, D., Gibelli, L., Townsend, P., & Vreugdenhil, B. J. (2016). Human behaviours in evacuation crowd dynamics: From modelling to “big data” toward crisis management. *Physics of Life Reviews*, 18, 1–21. <https://doi.org/10.1016/j.plrev.2016.05.014>
- Bendali-Braham, M., Weber, J., Forestier, G., Idoumghar, L., & Muller, P.-A. (2021). Recent trends in crowd analysis: A review. *Machine Learning with Applications*, 4, Article 100023. <https://doi.org/10.1016/j.mlwa.2021.100023>
- Blanke, U., Tröster, G., Franke, T., & Lukowicz, P. (2014). Capturing crowd dynamics at large scale events using participatory GPS-localization. *IEEE ISSNIP 2014 - 2014 IEEE 9th International Conference on Intelligent Sensors, Sensor Networks and Information Processing. Conference Proceedings*, (Section VI). 10.1109/ISSNIP.2014.6827652.
- Blondel, V. D., Esch, M., Chan, C., Clérot, F., Deville, P., Huens, E Ziemlicki, C. (2012). Data for development: the d4d challenge on mobile phone data. *ArXiv Preprint ArXiv: 1210.0137*.
- Boltes, M., Adrian, J., & Raytarowski, A. K. (2021). A hybrid tracking system of full-body motion inside crowds. *Sensors*, 21(6), 1–18. <https://doi.org/10.3390/s21062108>
- Borshchev, A. (2013). *The big book of simulation modeling: multimethod modeling with AnyLogic 6*. AnyLogic North America.
- Caramuta, C., Collodel, G., Giacomini, C., Gruden, C., Longo, G., & Piccolotto, P. (2017). Survey of detection techniques, mathematical models and simulation software in pedestrian dynamics. *Transportation Research Procedia*, 25, 551–567. <https://doi.org/10.1016/j.trpro.2017.05.438>
- Celes, C., Boukerche, A., & Loureiro, A. A. F. (2019). Crowd management: A new challenge for urban big data analytics. *IEEE Communications Magazine*, 57(4), 20–25. <https://doi.org/10.1109/MCOM.2019.1800640>
- Challenger, R., Clegg, C. W., & Robinson, M. A. (2009). Understanding crowd behaviours: Supporting evidence. *American Review of Canadian Studies*, 11. <https://doi.org/10.1080/02722018109480726>
- Challenger, R., Clegg, C. W., Robinson, M. A., & Leigh, M. (2009). Understanding crowd behaviours: simulation tools. *UK Cabinet Office*.
- Chan, A. B., Zhang-Sheng John Liang, & Vasconcelos, N. (2008). Privacy preserving crowd monitoring: Counting people without people models or tracking. In *2008 IEEE Conference on Computer Vision and Pattern Recognition* (pp. 1–7). IEEE. 10.1109/CVPR.2008.4587569.
- Chen, K., Loy, C. C., Gong, S., & Xiang, T. (2012). Feature Mining for Localised Crowd Counting. *Proceedings of the British Machine Vision Conference 2012*, 21.1-21.11. 10.5244/C.26.21.
- Courty, N., Allain, P., Creusot, C., & Corpetti, T. (2014). Using the agoraset dataset: Assessing for the quality of crowd video analysis methods. *Pattern Recognition Letters*, 44, 161–170. <https://doi.org/10.1016/j.patrec.2014.01.004>
- Dias, C. G. J. (2015). *Crowd dynamics at turning phenomena: experiments and modelling*. Monash University. Retrieved from [https://scholar.google.com/scholar?hl=en&as\\_sdt=0%2C5&q=+Crowd+Dynamics+at+Turning+Phenomena%3A+Experiments+and+Modelling&btnG=-](https://scholar.google.com/scholar?hl=en&as_sdt=0%2C5&q=+Crowd+Dynamics+at+Turning+Phenomena%3A+Experiments+and+Modelling&btnG=-).
- Draghici, A., & Steen, M. V. (2018). A survey of techniques for automatically sensing the behavior of a crowd. *ACM Computing Surveys*, 51(1), 1–40. <https://doi.org/10.1145/3129343>
- Dridi, M. H. (2015). Pedestrian flow simulation validation and verification techniques. *Current Urban Studies*, 03(02), 119–134.
- Dubroca-Voisin, M., Kabalan, B., & Leurent, F. (2019). On pedestrian traffic management in railway stations: Simulation needs and model assessment. *Transportation Research Procedia*, 37, 3–10. <https://doi.org/10.1016/j.trpro.2018.12.159>
- Dupont, C., Tobias, L., & Luvison, B. (2017). Crowd-11: A Dataset for Fine Grained Crowd Behaviour Analysis. In *IEEE Computer Society Conference on Computer Vision and Pattern Recognition Workshops* (Vol. 2017-July, pp. 2184–2191). 10.1109/CVPRW.2017.271.
- Felemban, E. A., Rehman, F. U., Biabani, S. A. A., Ahmad, A., Naseer, A., Majid, A. R. M. A., ... Zanjir, F. (2020). Digital revolution for hajj crowd management: A technology survey. *IEEE Access*, 8, 208583–208609. <https://doi.org/10.1109/ACCESS.2020.3037396>
- Feliciani, C., & Nishinari, K. (2018). Measurement of congestion and intrinsic risk in pedestrian crowds. *Transportation Research Part C: Emerging Technologies*, 91, 124–155. <https://doi.org/10.1016/j.trc.2018.03.027>
- Ferryman, J., & Shahrokni, A. (2009). PETS2009: Dataset and challenge. In *Proceedings of the 12th IEEE International Workshop on Performance Evaluation of Tracking and Surveillance, PETS-Winter 2009*. 10.1109/PETS-WINTER.2009.5399556.
- Franke, T., Lukowicz, P., & Blanke, U. (2015). Smart crowds in smart cities: Real life, city scale deployments of a smartphone based participatory crowd management platform. *Journal of Internet Services and Applications*, 6(1), 1–19. <https://doi.org/10.1186/s13174-015-0040-6>
- Fruin, J. (1981). Crowd disasters-a systems evaluation of causes and countermeasures. *Inc. US National Bureau of Standards, Pub. NBSIR*, 81–3261.
- Fruin, J. J. (1987). *Pedestrian Planning and Design*, Revised Edition. *Elevator World Educational, Services Division, Mobile, AL*. Retrieved from <https://trid.trb.org/view/114653>.
- Gloor, C. (2016). PEDSIM - Pedestrian Crowd Simulation. Retrieved July 2, 2019, from <http://pedsim.silmaril.org/>.
- Haghani, M., & Sarvi, M. (2018). Crowd behaviour and motion: Empirical methods. *Transportation Research Part B: Methodological*, 107, 253–294. <https://doi.org/10.1016/j.trb.2017.06.017>
- Hassner, T., Itcher, Y., & Kliper-Gross, O. (2012). Violent flows: Real-time detection of violent crowd behavior. In *IEEE Computer Society Conference on Computer Vision and Pattern Recognition Workshops* (pp. 1–6). IEEE. 10.1109/CVPRW.2012.6239348.

- Hawkins, J. (2014). The Science of Anomaly Detection. *Numenta, Inc.*, 1–18.
- Helbing, D., Brockmann, D., Chadefaux, T., Donnay, K., Blanke, U., Woolley-Meza, O., ... Perc, M. (2015). Saving human lives: What Complexity Science and Information Systems can Contribute. *Journal of Statistical Physics*, 158(3), 735–781. <https://doi.org/10.1007/s10955-014-1024-9>
- Helbing, D., Buzna, L., Johansson, A., & Werner, T. (2005). Self-organized pedestrian crowd dynamics: Experiments, simulations, and design solutions. *Transportation Science*, 39(1), 1–24. <https://doi.org/10.1287/trsc.1040.0108>
- Helbing, D., Farkas, I. J., Molnar, P., & Vicsek, T. (2002). Simulation of pedestrian crowds in normal and evacuation situations. *Pedestrian and Evacuation Dynamics*, 21(2), 21–58.
- Helbing, D., & Johansson, A. (2013). Pedestrian, Crowd, and Evacuation Dynamics. In *Encyclopedia of Complexity and Systems Science* (pp. 1–28). [https://doi.org/10.1007/978-3-642-27737-5\\_382-5](https://doi.org/10.1007/978-3-642-27737-5_382-5)
- Helbing, D., & Molnár, P. (1995a). Social force model for pedestrian dynamics. *Physical Review E*, 51(5), 4282–4286. <https://doi.org/10.1103/PhysRevE.51.4282>
- Helbing, D., & Molnár, P. (1995b). Social force model for pedestrian dynamics – Annotated. Retrieved from *Physical Review E*, 51(5), 5 <https://arxiv.org/pdf/c ond-mat/9805244.pdf>.
- Helbing, D., & Mukerji, P. (2012). Crowd Disasters as Systemic Failures: Analysis of the Love Parade Disaster, 1–40. 10.1140/epjds7.
- Hesham, O., & Wainer, G. (2021). Advanced models for centroidal particle dynamics: Short-range collision avoidance in dense crowds. *Simulation*, 97(8), 529–543. <https://doi.org/10.1177/00375497211003126>
- Higuchi, T., Yamaguchi, H., & Higashino, T. (2015). Mobile devices as an infrastructure: A survey of opportunistic sensing technology. *Journal of Information Processing*, 23(2), 94–104. <https://doi.org/10.2197/ipsjip.23.94>
- Hochreiter, S., & Schmidhuber, J. (1997). Long short-term memory. *Neural computation*, 9(8), 1735–1780.
- Ibrahim, A. M., Venkat, I., Subramanian, K. G., Khader, A. T., & Wilde, P. D. (2016). Intelligent Evacuation Management Systems. *ACM Transactions on Intelligent Systems and Technology*, 7(3), 1–27. <https://doi.org/10.1145/2842630>
- Idrees, H., Saleemi, I., Seibert, C., & Shah, M. (2013). Multi-source multi-scale counting in extremely dense crowd images. In *In Proceedings of the IEEE Computer Society Conference on Computer Vision and Pattern Recognition* (pp. 2547–2554). <https://doi.org/10.1109/CVPR.2013.329>
- Irfan, M., Tokarchuk, L., Marcenaro, L., & Regazzoni, C. (2018). ANOMALY DETECTION IN CROWDS USING MULTI SENSORY INFORMATION. In *In 2018 15th IEEE International Conference on Advanced Video and Signal Based Surveillance (AVSS)* (pp. 1–6). <https://doi.org/10.1109/AVSS.2018.8639151>
- Jin, B., Wang, J., Wang, Y., Gu, Y., & Wang, Z. (2020). Temporal and spatial distribution of pedestrians in subway evacuation under node failure by multi-hazards. *Safety Science*, 127. <https://doi.org/10.1016/j.ssci.2020.104695>
- Jin, W., Tung, A. K. H., Han, J., & Wang, W. (2006). Ranking outliers using symmetric neighborhood relationship. In *Lecture Notes in Computer Science (including subseries Lecture Notes in Artificial Intelligence and Lecture Notes in Bioinformatics)* (Vol. 3918 LNAI, pp. 577–593). [https://doi.org/10.1007/11731139\\_68](https://doi.org/10.1007/11731139_68).
- Johansson, A., Helbing, D., Al-Abideen, H. Z., & Al-Bosta, S. (2008a). From crowd dynamics to crowd safety: A video-based analysis. *Advances in Complex Systems*, 11(04), 497–527.
- Johansson, A., Helbing, D., Al-Abideen, H. Z., & Al-Bosta, S. (2008b). *From Crowd Dynamics to Crowd Safety: A Video-Based Analysis*. <https://doi.org/10.1142/S0219525908001854>
- Kaiser, M. S., Lwin, K. T., Mahmud, M., Hajjalizadeh, D., Chaipimolpin, T., Sarhan, A., & Hossain, M. A. (2018). Advances in crowd analysis for urban applications through urban event detection. *IEEE Transactions on Intelligent Transportation Systems*, 19(10), 3092–3112. <https://doi.org/10.1109/ITITS.2017.2771746>
- Khadka, A. R., Oghaz, M. M., Matta, W., Cosentino, M., Remagnino, P., & Argyriou, V. (2019). Learning how to analyse crowd behaviour using synthetic data. In *In ACM International Conference Proceeding Series* (pp. 11–14). <https://doi.org/10.1145/3328756.3328773>
- Khan, K., Albattah, W., Khan, R. U., Qamar, A. M., & Nayab, D. (2020). Advances and trends in real time visual crowd analysis. *Sensors (Basel, Switzerland)*, 20(18), 1–28. <https://doi.org/10.3390/s20185073>
- Khan, S. D. (2019). Congestion detection in pedestrian crowds using oscillation in motion trajectories. *Engineering Applications of Artificial Intelligence*, 85, 429–443. <https://doi.org/10.1016/j.engappai.2019.07.009>
- Kinsey, M., Walker, G., Swales, N., & Butterworth, N. (2015). *The Verification and Validation of MassMotion for Evacuation Modelling*. Retrieved from <https://www.oasys-software.com/wp-content/uploads/2017/11/The-Verification-and-Validation-of-MassMotion-for-Evacuation-Modelling-Report.pdf>.
- Kok, V. J., Lim, M. K., & Chan, C. S. (2016). Crowd behavior analysis: A review where physics meets biology. *Neurocomputing*, 177, 342–362. <https://doi.org/10.1016/j.neucom.2015.11.021>
- Kretz, T. (2011). A level of service scheme for microscopic simulation of pedestrians that integrates queuing, uni-and multi-directional flow situations. *European Transport Research Review*, 3(4), 211–220. <https://doi.org/10.1007/s12544-011-0060-7>
- Kriegel, H. P., Kröger, P., Schubert, E., & Zimek, A. (2009). LoOP: Local outlier probabilities. In *In International Conference on Information and Knowledge Management, Proceedings* (pp. 1649–1652). <https://doi.org/10.1145/1645953.1646195>
- Krithigaran, R., & Karthik, R. (2014). An enhanced detection of outlier using independent component analysis among multiple data instances via oversampling. *IOSR Journal of Computer Engineering*, 16(2), 31–34. <https://doi.org/10.9790/0661-16283134>
- Kuligowski, E. D., Peacock, R. D., & Hoskins, B. L. (2010). Technical Note 1680 A Review of Building Evacuation Models , 2nd Edition. *Secretary*.
- Kumar, N., & Nasser, M. (2012). A new graphical multivariate outlier detection technique using singular value decomposition. *International Journal of Engineering Research & Technology*, 1(6), 1–6. Retrieved from [www.ijert.org](http://www.ijert.org).
- LeCun, Y., Bottou, L., Bengio, Y., & Haffner, P. (1998). Gradient-based learning applied to document recognition. *Proceedings of the IEEE*, 86(11), 2278–2324.
- Li, L., Wei, L. L., Kinsey, M., & Sun, A. (2018). HSTEAM - High Speed Train Evacuation Analysis Methodology. In *Procedia Engineering* (Vol. 211, pp. 18–27). Elsevier Ltd. 10.1016/j.proeng.2017.12.133.
- Li, T., Chang, H., Wang, M., Ni, B. B., Hong, R. C., & Yan, S. C. (2015). Crowded scene analysis: A survey. *IEEE Transactions on Circuits and Systems for Video Technology*, 25(3), 367–386. <https://doi.org/10.1109/Tcsvt.2014.2358029>
- Li, W., Mahadevan, V., & Vasconcelos, N. (2013). Anomaly detection and localization in crowded scenes. *IEEE Transactions on Pattern Analysis and Machine Intelligence*, 36(1), 18–32.
- Li, X., Yu, Q., Alzahrani, B., Barnawi, A., Alhindi, A., Alghazzawi, D., & Miao, Y. (2021). Data fusion for intelligent crowd monitoring and management systems: A survey. *IEEE Access*. <https://doi.org/10.1109/ACCESS.2021.3060631>
- Liu, Y., Hao, K., Tang, X., & Wang, T. (2019). Abnormal Crowd Behavior Detection Based on Predictive Neural Network. In *Proceedings of 2019 IEEE International Conference on Artificial Intelligence and Computer Applications, ICAICA 2019* (pp. 221–225). Institute of Electrical and Electronics Engineers Inc. 10.1109/ICAICA.2019.8873488.
- Luque Sánchez, F., Hupont, I., Tabik, S., & Herrera, F. (2020). Revisiting crowd behaviour analysis through deep learning: Taxonomy, anomaly detection, crowd emotions, datasets, opportunities and prospects. *Information Fusion*, 64, 318–335. <https://doi.org/10.1016/j.inffus.2020.07.008>
- Mehran, R., Oyama, A., & Shah, M. (2009). Abnormal crowd behavior detection using social force model, 935–942. 10.1109/CVPR.2009.5206641.
- Mohamed, M. F., Shabayek, A. E. R., & El-Gayyar, M. (2019). IoT-based framework for crowd management. In *EAI/Springer Innovations in Communication and Computing* (pp. 47–61). Springer Science and Business Media Deutschland GmbH. 10.1007/978-3-319-93491-4\_3.
- Musolesi, M., Fodor, K., Piraccini, M., Corradi, A., & Campbell, A. (2008). CRAWDAD dataset dartmouth/cenceme (v.2008-08-13). *CRAWDAD Wireless Network Data Archive*. Doi: 10.15783/C76P4X.
- Neufert, E. (2002). *Neufert. Architects' Data. Third Edition Edited by B. Baiche, N. Walliman*, 636.
- O'Donnell, D., Roberts, T., & Debney, P. (2017). *MassMotion - A step in the right direction*. <https://doi.org/10.1016/j.gaitpost.2005.01.004>.
- Oasys. (2019). *MassMotion Help Guide*. Retrieved from <http://www.oasys-software.com/>.
- Oberhagemann, D. (2012). Static and Dynamic Crowd Densities at Major Public Events. *Technisch-Wissenschaftlicher Beirat (TWB) Der*, (March), 1–48.
- Polus, A., Schofer, J. L., & Ushpiz, A. (1983). Pedestrian flow and level of service. *Journal of Transportation Engineering*, 109(1), 46–56. [https://doi.org/10.1061/\(ASCE\)0733-947X\(1983\)109:1\(46\)](https://doi.org/10.1061/(ASCE)0733-947X(1983)109:1(46))
- Purdy, S. (2016). Encoding Data for HTM Systems. Retrieved from <http://arxiv.org/abs/1602.05925>.
- Ruggiero, L., Charitha, D., Xiang, S., & Lucia, B. (2018). Investigating pedestrian navigation in indoor open space environments using big data. *Applied Mathematical Modelling*, 62, 499–509. <https://doi.org/10.1016/j.apm.2018.06.014>
- Saleh, S. A. M., Suandi, S. A., & Ibrahim, H. (2015). Recent survey on crowd density estimation and counting for visual surveillance. *Engineering Applications of Artificial Intelligence*, 41, 103–114. <https://doi.org/10.1016/j.engappai.2015.01.007>
- Savannah Simulations AG. (2017). *SimWalk User Guide*. Retrieved from [https://www.simwalk.com/modules/simwalk\\_roadtraffic.html](https://www.simwalk.com/modules/simwalk_roadtraffic.html).
- Schauer, L., Werner, M., & Marcus, P. (2014). Estimating Crowd Densities and Pedestrian Flows Using Wi-Fi and Bluetooth. *Proceedings of the 11th International Conference on Mobile and Ubiquitous Systems: Computing, Networking and Services*, 171–177. 10.4108/icst.mobiquitous.2014.257870.
- Shao, J., Kang, K., Loy, C. C., & Wang, X. (2015). Deeply learned attributes for crowded scene understanding. In *Proceedings of the IEEE Computer Society Conference on Computer Vision and Pattern Recognition* (Vol. 07-12-June, pp. 4657–4666). 10.1109/CVPR.2015.7299097.
- Shao, J., Loy, C. C., & Wang, X. (2014). Scene-independent group profiling in crowd. In *Proceedings of the IEEE Computer Society Conference on Computer Vision and Pattern Recognition* (pp. 2227–2234). 10.1109/CVPR.2014.285.
- SIMWALK. (1996). *SIMWALK – Pedestrian Database with all the data needed for pedestrian modelling and simulation*. Retrieved February 17, 2021, from <https://www.simwalk.com/modules/index.html>.
- Sindagi, V., Yasarla, R., & Patel, V. M. M. (2020). JHU-CROWD++: Large-Scale Crowd Counting Dataset and A Benchmark Method. *IEEE Transactions on Pattern Analysis and Machine Intelligence*. <https://doi.org/10.1109/TPAMI.2020.3035969>
- Smith, R. A. (1995). Density, velocity and flow relationships for closely packed crowds. *Safety Science*, 18(4), 321–327. [https://doi.org/10.1016/0925-7535\(94\)00051-4](https://doi.org/10.1016/0925-7535(94)00051-4)
- Still, G. Keith. (2000). PhD Chapter 5 - Legion. Retrieved February 17, 2021, from <https://www.gkstill.com/CV/PhD/Chapter5.html>.
- Still, G. Keith. (2011). Moving Crowd Density. Retrieved March 19, 2022, from <https://www.gkstill.com/Support/crowd-flow/MovingDensity.html>.
- Still, G.K. (2004). Crowd Dynamics, Crowd Management, Crowd Modelling, Crowd Behaviour. Retrieved July 4, 2019, from <http://www.crowddynamics.com/>.
- Still, K. (2011). Standing Crowd Density. Retrieved March 19, 2022, from <https://www.gkstill.com/Support/crowd-density/CrowdDensity-1.html>.
- Tissue, S., & Wilensky, U. (2004). NetLogo: A simple environment for modeling complexity. In *International conference on complex systems* (Vol. 21, pp. 16–21).

- Toto, E., Rundensteiner, E. A., Li, Y., Jordan, R., Ishutkina, M., Claypool, K., ... Zhang, F. (2016). PULSE: A real time system for crowd flow prediction at metropolitan subway stations. In *Lecture Notes in Computer Science (including subseries Lecture Notes in Artificial Intelligence and Lecture Notes in Bioinformatics)* (Vol. 9853 LNCS, pp. 112–128). 10.1007/978-3-319-46131-1\_19.
- UCSD. (2010). UCSD Anomaly Detection Dataset. Retrieved February 17, 2021, from <http://www.svcl.ucsd.edu/projects/anomaly/dataset.htm>.
- University of Central Florida. (2011a). CRCV | Center for Research in Computer Vision at the University of Central Florida. Retrieved September 10, 2019, from <https://www.crcv.ucf.edu/data/>.
- van der Steen, J., & Boardman, T. (2012). Rendering with mental ray and 3ds Max. In *Rendering with mental ray and 3ds Max* (pp. 23–62). 10.4324/9780240813905-6.
- Vermuyten, H., Beliën, J., De Boeck, L., Reniers, G., & Wauters, T. (2016). A review of optimisation models for pedestrian evacuation and design problems. *Safety Science*, 87, 167–178. <https://doi.org/10.1016/j.ssci.2016.04.001>
- Wang, Q., Gao, J., Lin, W., & Li, X. (2020). NWPU-crowd: A large-scale benchmark for crowd counting and localization. *IEEE Transactions on Pattern Analysis and Machine Intelligence*.
- Wang, Q., Gao, J., Lin, W., & Yuan, Y. (2019). Learning from synthetic data for crowd counting in the wild. In *Proceedings of the IEEE Computer Society Conference on Computer Vision and Pattern Recognition* (Vol. 2019-June, pp. 8190–8199). 10.1109/CVPR.2019.00839.
- Wilensky, U. (2012). NetLogo. Retrieved February 17, 2021, from <https://ccl.northwestern.edu/netlogo/>.
- Wirz, M., Franke, T., Roggen, D., Mitleton-Kelly, E., Lukowicz, P., & Tröster, G. (2012). Inferring crowd conditions from pedestrians' location traces for real-time crowd monitoring during city-scale mass gatherings. In *In 2012 IEEE 21st International Workshop on Enabling Technologies: Infrastructure for Collaborative Enterprises* (pp. 367–372). <https://doi.org/10.1109/WETICE.2012.26>
- Wirz, M., Franke, T., Roggen, D., Mitleton-Kelly, E., Lukowicz, P., & Tröster, G. (2013). Probing crowd density through smartphones in city-scale mass gatherings. *EPJ Data Science*, 2(1), 1–24. <https://doi.org/10.1140/epjds17>
- Wu, X., Dong, Y., Huang, C., Xu, J., Wang, D., & Chawla, N. V. (2017). UAPD: Predicting Urban Anomalies from Spatial-Temporal Data. In *Lecture Notes in Computer Science (including subseries Lecture Notes in Artificial Intelligence and Lecture Notes in Bioinformatics)* (Vol. 10535 LNAI, pp. 622–638). 10.1007/978-3-319-71246-8\_38.
- Xie, P., Li, T., Liu, J., Du, S., Yang, X., & Zhang, J. (2020). Urban flow prediction from spatiotemporal data using machine learning: A survey. *Information Fusion*, 59, 1–12. <https://doi.org/10.1016/j.inffus.2020.01.002>
- Yang, S., Li, T., Gong, X., Peng, B., & Hu, J. (2020). A review on crowd simulation and modeling. *Graphical Models*, 111, Article 101081. <https://doi.org/10.1016/j.gmod.2020.101081>
- Zawbaa, H., & Aly, S. A. (2012). Hajj and umrah event recognition datasets. *ArXiv Preprint ArXiv:1205.2345*. Retrieved from <https://arxiv.org/abs/1205.2345v1>.
- Zhang, C., Kang, K., Li, H., Wang, X., Xie, R., & Yang, X. (2016). Data-driven crowd understanding: A baseline for a large-scale crowd dataset. *IEEE Transactions on Multimedia*, 18(6), 1048–1061. <https://doi.org/10.1109/TMM.2016.2542585>
- Zhang, M., Li, T., Yu, Y., Li, Y., Hui, P., & Zheng, Y. (2020). Urban anomaly analytics: Description, detection and prediction. *IEEE Transactions on Big Data*, 1–1. <https://doi.org/10.1109/TBDDATA.2020.2991008>
- Zhang, X., Yu, Q., & Yu, H. (2018). Physics inspired methods for crowd video surveillance and analysis: A survey. *IEEE Access*, 6, 66816–66830. <https://doi.org/10.1109/ACCESS.2018.2878733>
- Zhang, Y., Zhou, D., Chen, S., Gao, S., & Ma, Y. (2016). Single-image crowd counting via multi-column convolutional neural network. In *Proceedings of the IEEE Computer Society Conference on Computer Vision and Pattern Recognition* (Vol. 2016-December, pp. 589–597). 10.1109/CVPR.2016.70.
- Zhou, B., Tang, X., & Wang, X. (2013). Measuring crowd collectiveness. In *Proceedings of the IEEE Computer Society Conference on Computer Vision and Pattern Recognition* (pp. 3049–3056). <https://doi.org/10.1109/CVPR.2013.392>.
- Zhou, M., Dong, H., Ioannou, P. A., Zhao, Y., & Wang, F. Y. (2019, September 1). Guided crowd evacuation: Approaches and challenges. *IEEE/CAA Journal of Automatica Sinica*. Institute of Electrical and Electronics Engineers Inc. 10.1109/JAS.2019.1911672.
- Zitouni, M. S., Sluzek, A., & Bhaskar, H. (2019). Visual analysis of socio-cognitive crowd behaviors for surveillance: A survey and categorization of trends and methods. *Engineering Applications of Artificial Intelligence*, 82, 294–312. <https://doi.org/10.1016/j.engappai.2019.04.012>